Rank-one projection models in optics: from lensless interferometry to optical sketching

Laurent Jacques

INMA, ICTEAM, UCLouvain, Belgium

Frugalité et apprentissage machine

September 11, 2023.

ENS Lyon, France

Brief introduction

The multiple use of random projections in "data science"

Object

"$\boldsymbol{x}$"

signal
audio
image
volume
distribution
measure

$\mathcal{A}$ →

Random projection

$\boldsymbol{y} = \mathcal{A}(\boldsymbol{x})$

smaller dimension
physics-driven
distinctive
compressed
binarized

Random "projections" are ubiquitous in:

- Data mining & dimensionality reduction techniques
- Sensing and imaging methods (optics, astronomy, ...)
- Machine learning (sketching, explicit kernel, initialization, ...)
- Randomized numerical methods
- ...

Johnson-Lindenstrauss lemma (1984)

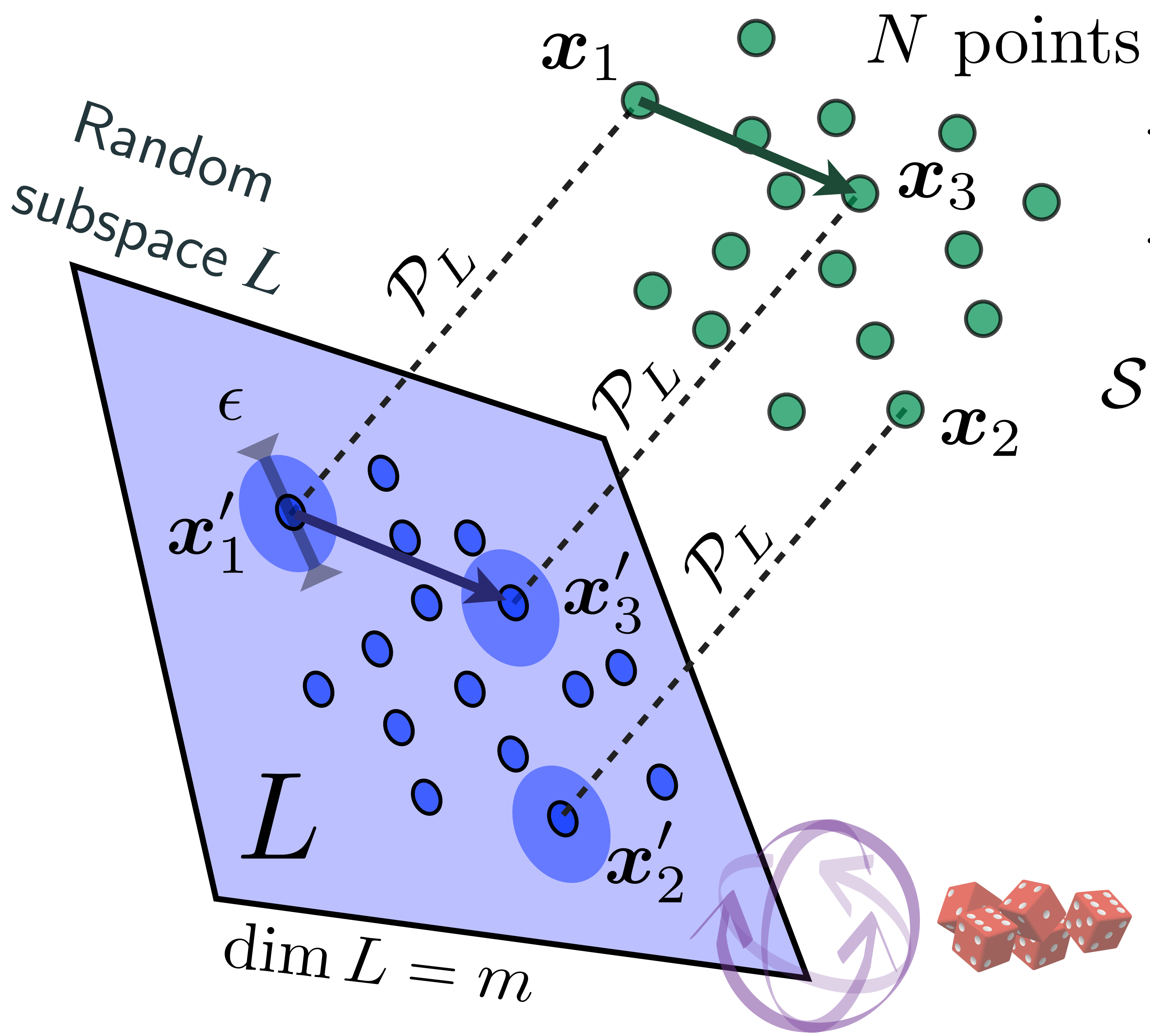

$\mathbb{R}^n$

$\mathcal{S} = \{\boldsymbol{x}_i : 1 \leqslant i \leqslant N\}$

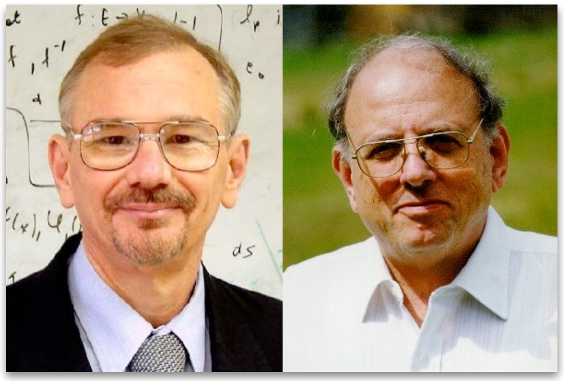

Johnson & Lindenstrauss

$m \geq \frac{C}{\epsilon^2} \log N \quad \Rightarrow \quad \|\boldsymbol{x}'_i - \boldsymbol{x}'_j\| \approx_\epsilon \|\boldsymbol{x}_i - \boldsymbol{x}_j\|$ (w.h.p. = with high probability)

↓ error (ϵ)

Embedding of sparse vectors / signals

Two K-sparse signals $\boldsymbol{x}, \boldsymbol{x}' \in \Sigma_K := \{\boldsymbol{u} : \|\boldsymbol{u}\|_0 := |\operatorname{supp} \boldsymbol{u}| \leqslant K\}$

At most K non-zero elements

For many random $M \times N$ matrices $\boldsymbol{\Phi}$ (e.g., Gaussian, Bernoulli, structured) and "$M \gtrsim K \log(N/K)$", with high probability,

Geometry of $\boldsymbol{\Phi}(\Sigma_K)$
$\approx$ Geometry of Σ_K

$$\boldsymbol{\Phi x} \approx \boldsymbol{\Phi x}' \Leftrightarrow \boldsymbol{x} \approx \boldsymbol{x}'$$

observations — true signals

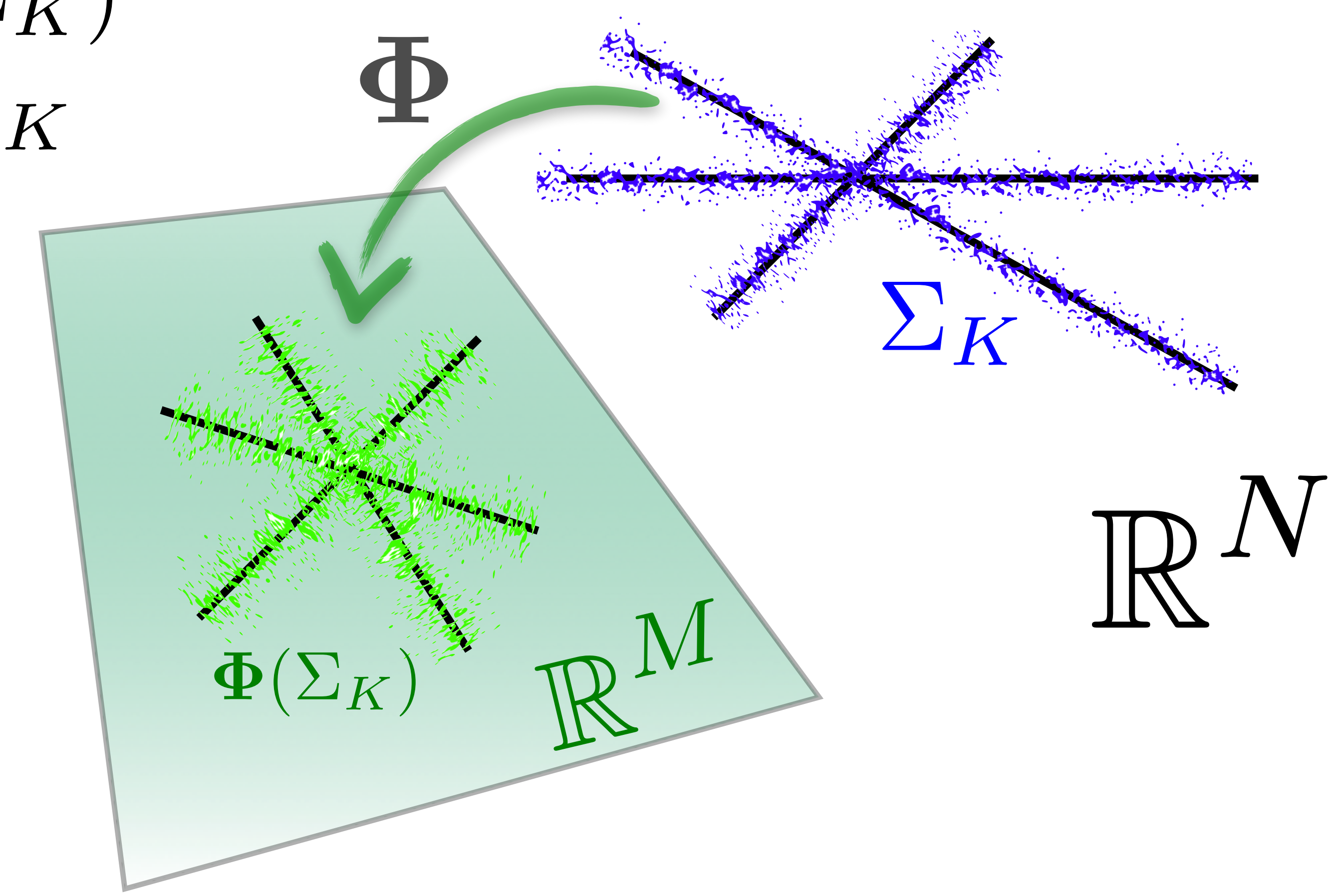

Embedding of low-complexity "objects"

Two low-complexity signals $\boldsymbol{x}, \boldsymbol{x}' \in \mathcal{K}$ (e.g., low-rank data 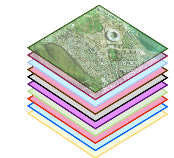)

For many random $M \times N$ matrices $\boldsymbol{\Phi}$ (e.g., Gaussian, Bernoulli, structured) and "$M \gtrsim C_{\mathcal{K}}$", with high probability,

Geometry of $\boldsymbol{\Phi}(\mathcal{K})$
$\approx$ Geometry of $\mathcal{K}$

$$\boldsymbol{\Phi x} \approx \boldsymbol{\Phi x}' \;\Leftrightarrow\; \boldsymbol{x} \approx \boldsymbol{x}'$$

observations — true signals

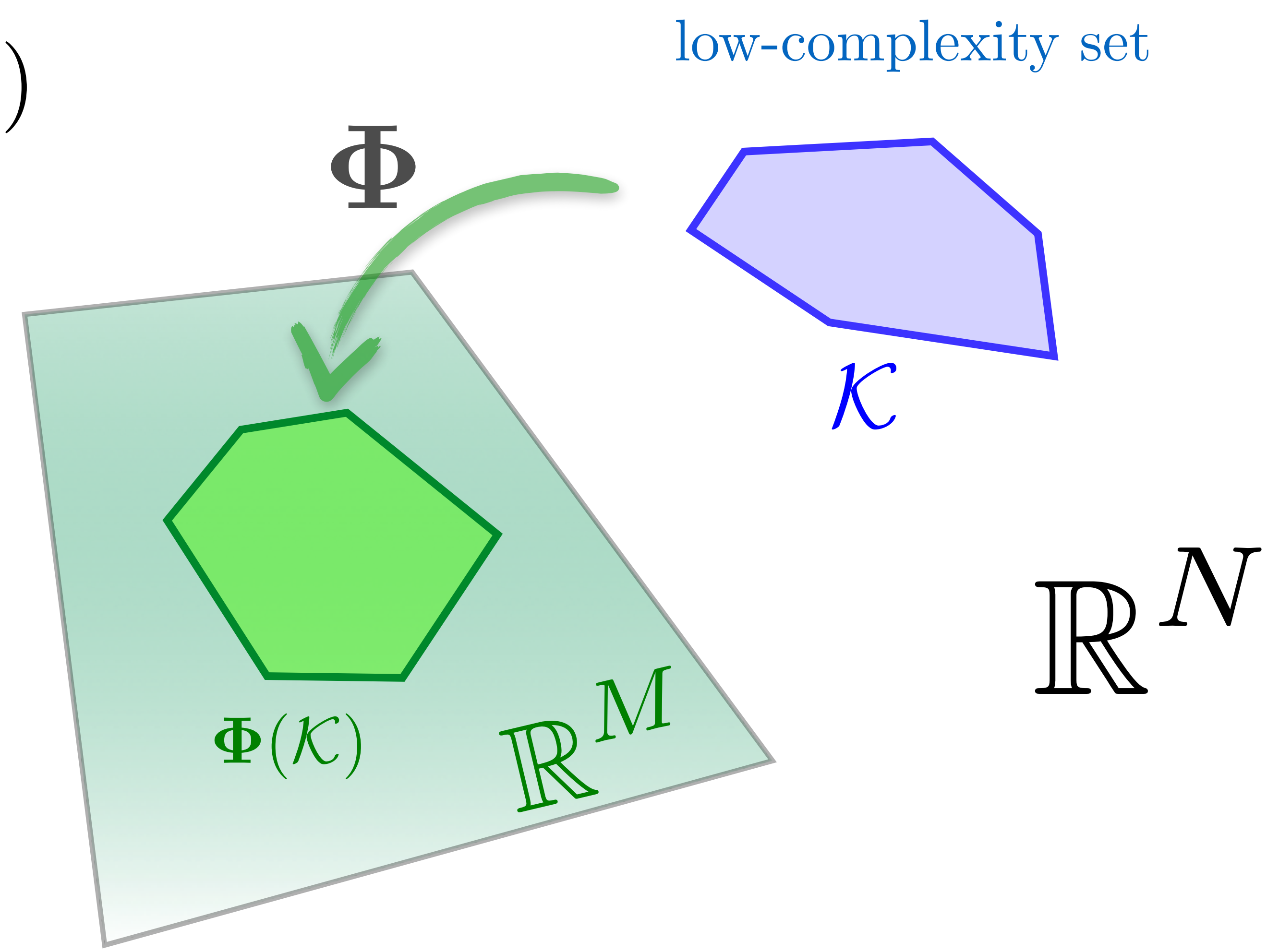

with $C_{\mathcal{K}} \equiv$ a dimension of $\mathcal{K}$ (*e.g.*, Gaussian width)

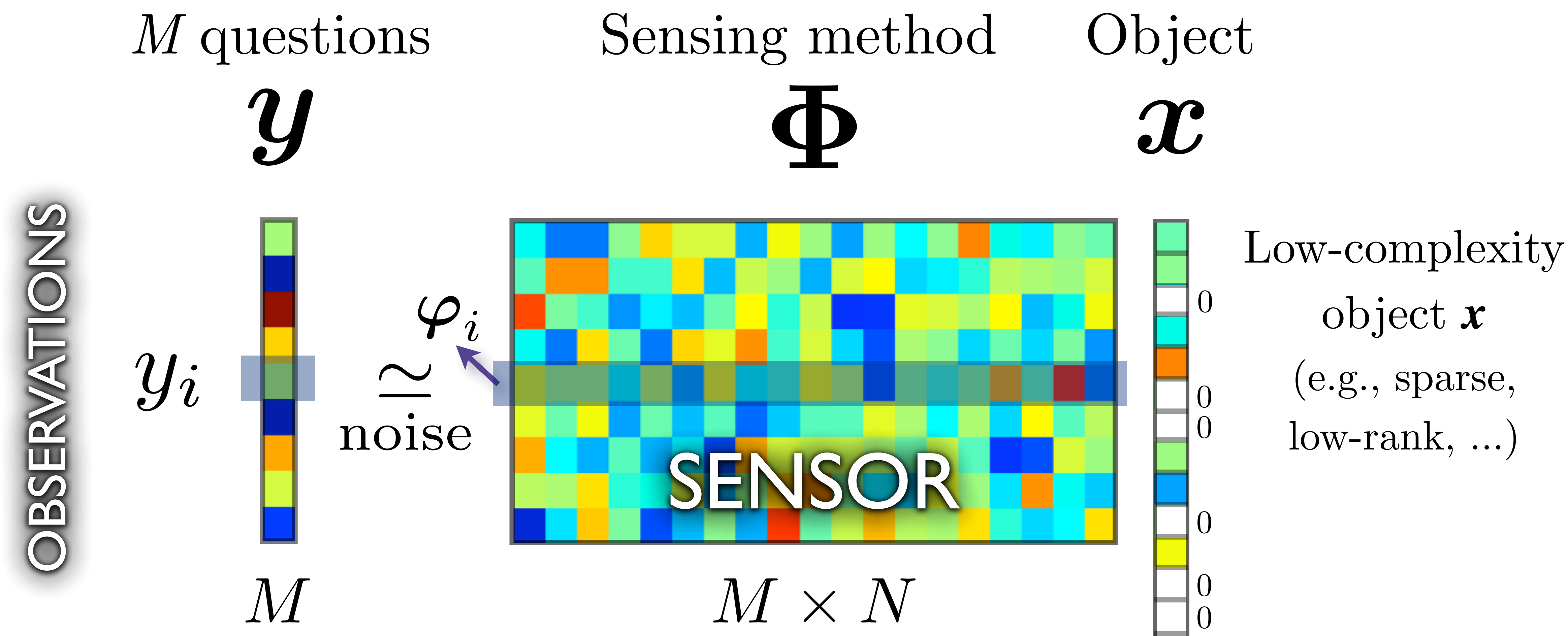

N

Generalized linear sensing!

$$y_i \simeq \langle \boldsymbol{\varphi}_i, \boldsymbol{x} \rangle = \boldsymbol{\varphi}_i^T \boldsymbol{x} \qquad 1 \leq i \leq M$$

e.g., to be realized optically/analogically

Generalized (non-linear) reconstruction

with regularized optimisation, greedy/iterative algorithms, ...

Structured random projections

Challenge: dense matrices $\boldsymbol{\Phi}$ not optimal for:

- memory and computational complexity
- physically friendly implementation
- sensing higher dimensional objects

Solution: simpler, structured projections based on

- Fourier (FFT) or Hadamard matrices

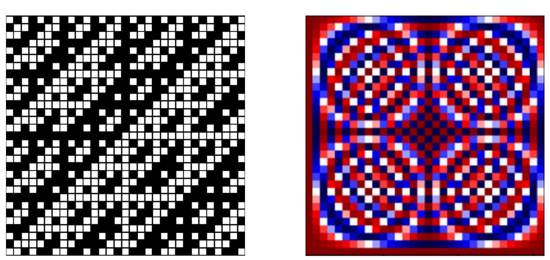

→ random subsampling & modulation → $\boldsymbol{\Phi}$

- Rank-one projections (ROP) 

Rank-one projections

Objects to project = symmetric $n \times n$ matrices $\boldsymbol{X}$

Projection with m random vectors $\{\boldsymbol{a}_j\}_{j=1}^m \subset \mathbb{R}^n$ (e.g., Gaussian)

$$\mathcal{A} : \boldsymbol{X} \in \mathbb{R}^{n \times n} \quad \mapsto \quad \boldsymbol{y} := \mathcal{A}(\boldsymbol{X}) := (\underbrace{\boldsymbol{a}_j^\top \boldsymbol{X} \boldsymbol{a}_j}_{\langle \boldsymbol{a}_j \boldsymbol{a}_j^\top, \boldsymbol{X} \rangle_F})_{j=1}^m \in \mathbb{R}^m$$

rank-one: $\boldsymbol{a}_j \boldsymbol{a}_j^\top$

+ extension to higher dimensional objects (tensors)

For low-complexity matrices (e.g., low-rank, Toeplitz, sparse, ...)

we can recover $\boldsymbol{X}$ from $\boldsymbol{y}$ with regularized optimization

+ error bounds and theoretical guarantees

Chen & Goldsmith (2015) Cai & Zhang (2015)

Rank-one projections

Applications:

- phase retrieval:

$$\boldsymbol{x} \quad \rightarrow \quad \underbrace{|\langle \boldsymbol{\varphi}_k, \boldsymbol{x}\rangle|^2}_{\text{intensity measurement}} = \boldsymbol{\varphi}_k^* \underbrace{(\boldsymbol{x}\boldsymbol{x}^*)}_{\boldsymbol{X}} \boldsymbol{\varphi}_k$$

  e.g., X-ray imaging, ptychography, ...

- covariance estimation: $\{\boldsymbol{x}_k\}_{j=1}^N \subset \mathbb{R}^n$ with $\mathbb{E}\, \boldsymbol{x}_k \boldsymbol{x}_k^\top = \Sigma$

$$\rightarrow \text{estimate } \Sigma \text{ from } \mathcal{A}\Big(\frac{1}{N}\sum_k \boldsymbol{x}_k \boldsymbol{x}_k\Big) = \frac{1}{N}\sum_k \underbrace{[(\boldsymbol{a}_j^\top \boldsymbol{x}_k)^2]_{j=1}^m}_{\text{``}(\boldsymbol{A}\boldsymbol{x}_j)^2\text{''}}$$

- and others (see later)

Chen & Goldsmith (2015) Cai & Zhang (2015)

Lensless interferometry & ROP

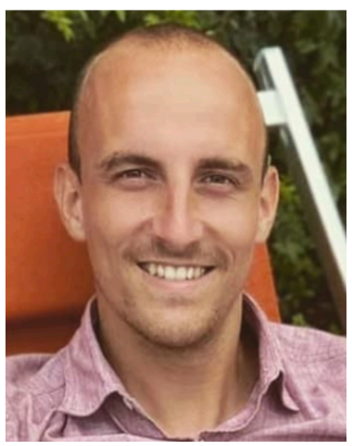

O. Leblanc[*]

L. Jacques[*]

M. Hofer[†]

H. Rigneault[†]

S. Sivankutty[‡]

[*]: ISPGroup, INMA, UCLouvain, Belgium. [†]: Institut Fresnel, France. [‡]: PhLAM, France.

How to see neurons firing?

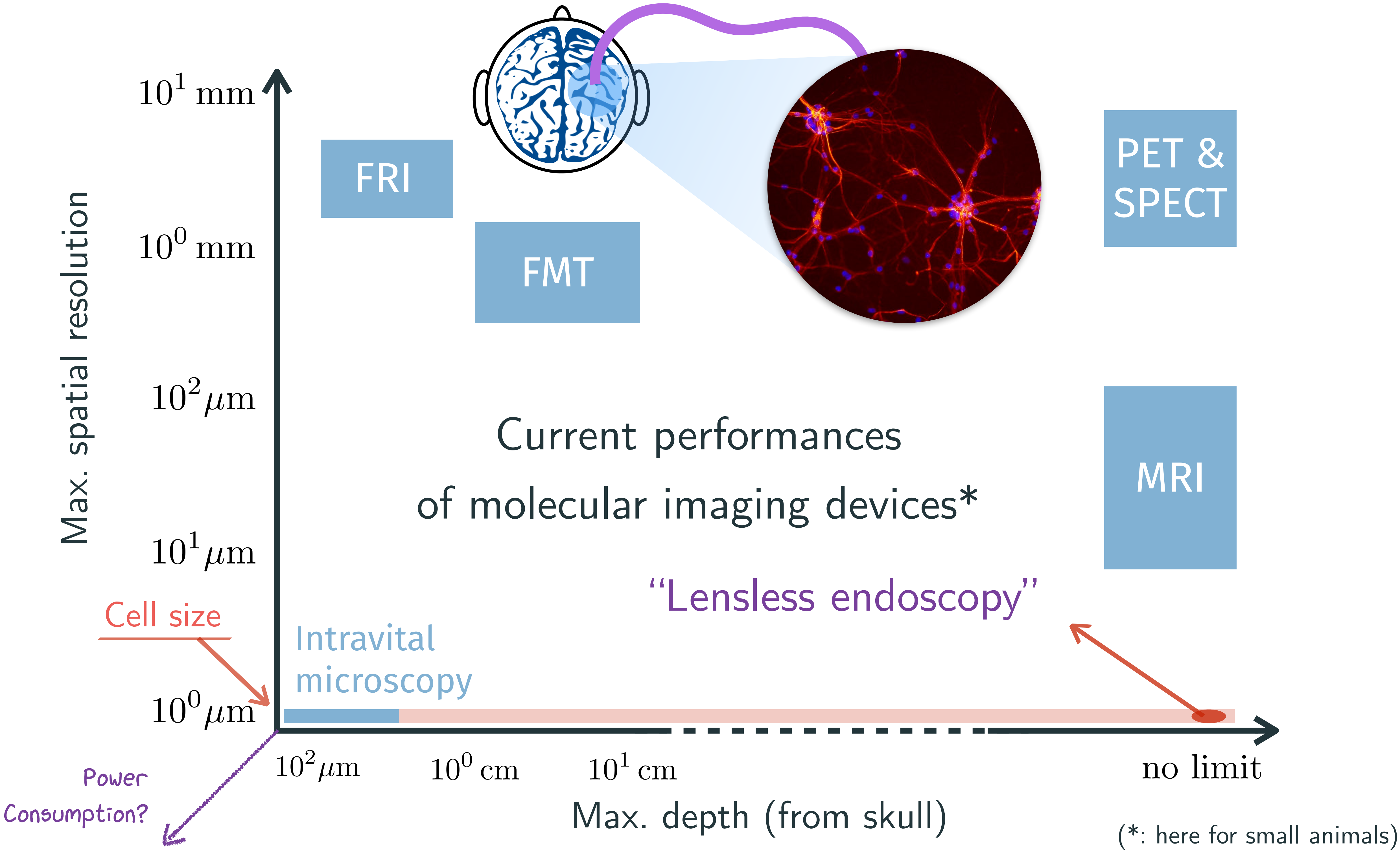

Rudin, M., & Weissleder, R. (2003). Molecular imaging in drug discovery and development. *Nature reviews Drug discovery*, *2*(2), 123-131.

Lensless endoscopy: focused mode

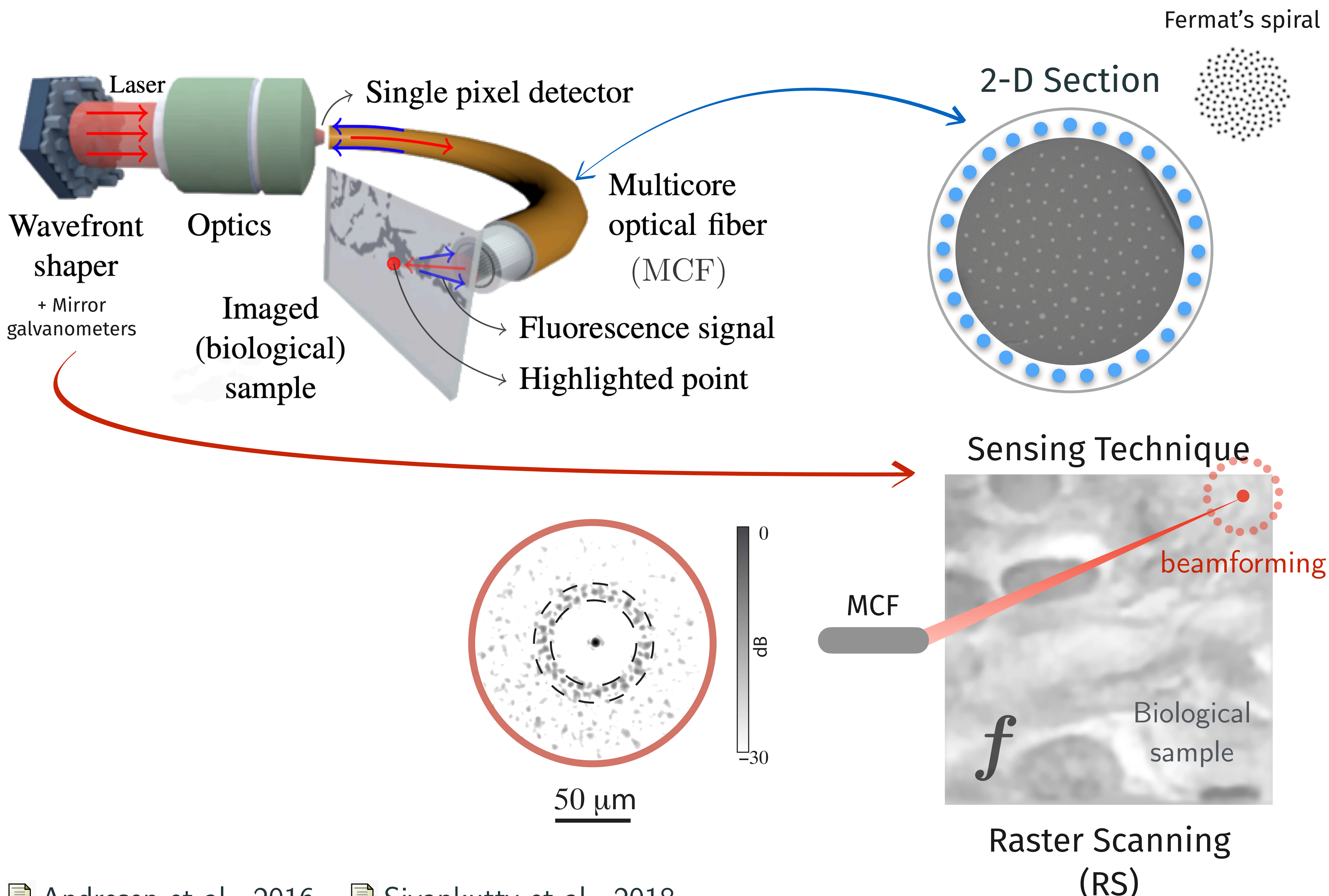

Andresen et al., 2016. Sivankutty et al., 2018.

Lensless endoscopy: focused mode

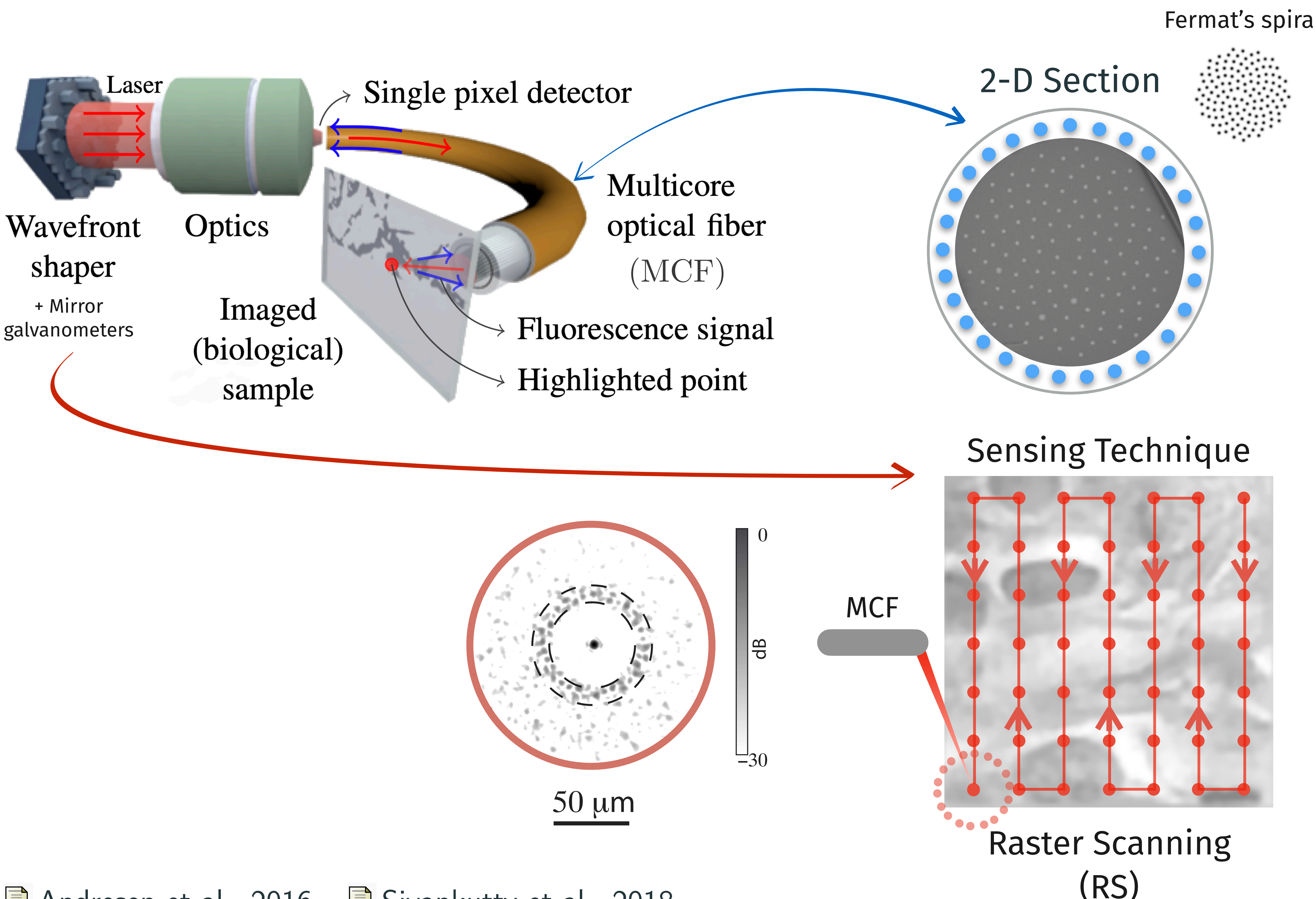

Andresen et al., 2016. Sivankutty et al., 2018.

Lensless endoscopy: focused mode

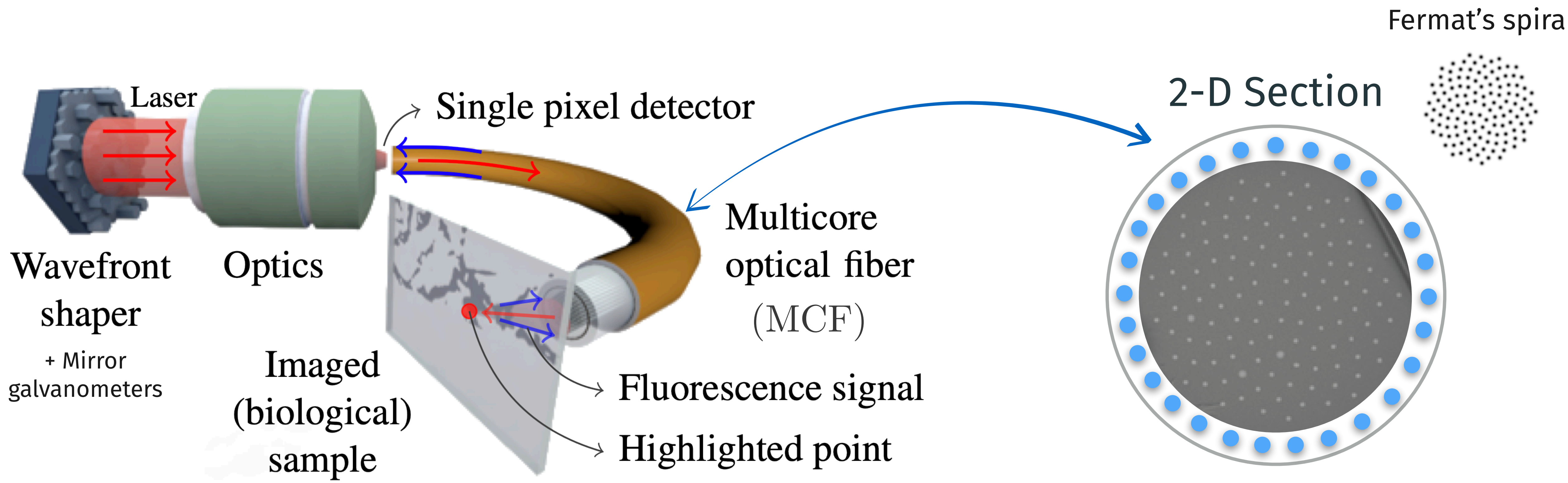

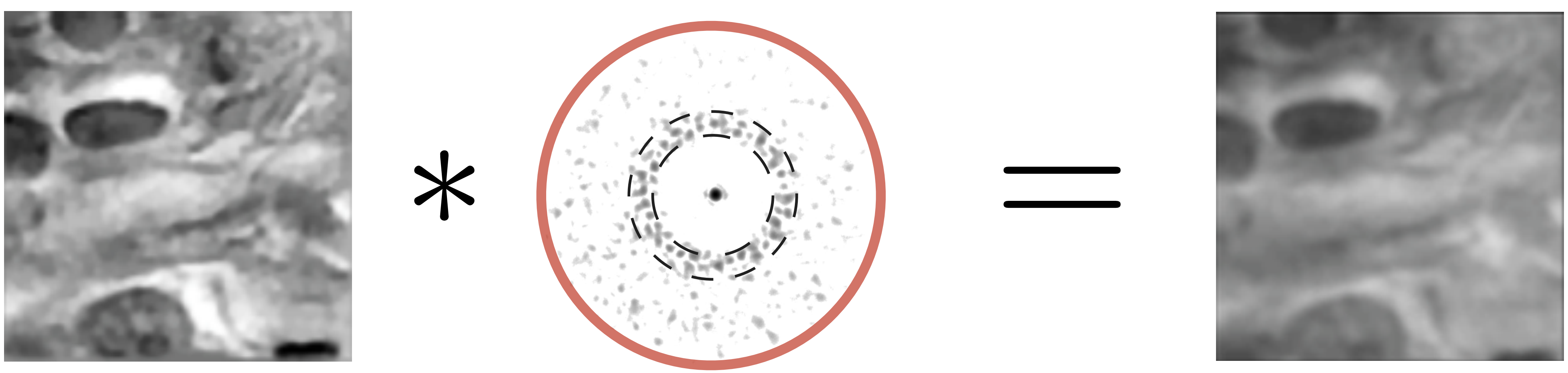

Sensing model

Direct Imaging
(+ possible deconvolution)

A closer look to sensing model

Back to the model...

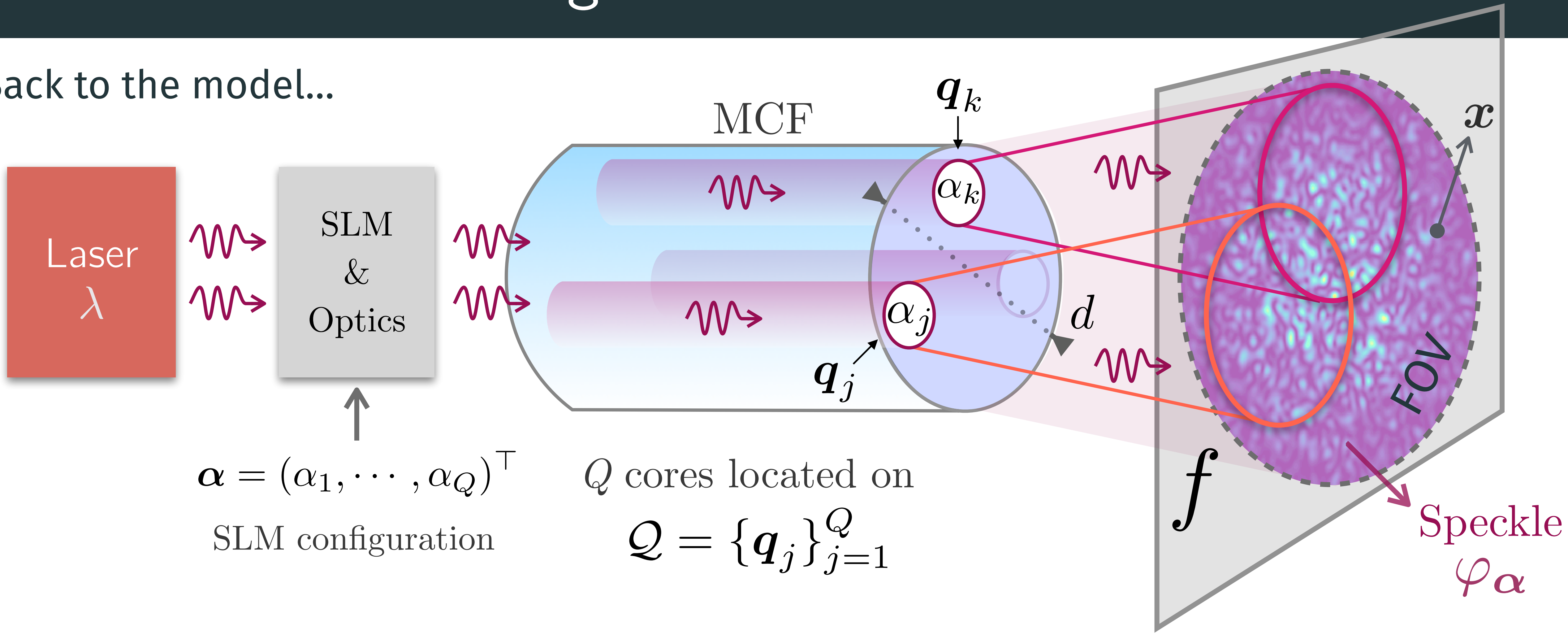

$\boldsymbol{\alpha} = (\alpha_1, \cdots, \alpha_Q)^\top$

SLM configuration

Q cores located on

$\mathcal{Q} = \{\boldsymbol{q}_j\}_{j=1}^{Q}$

Back to the model...

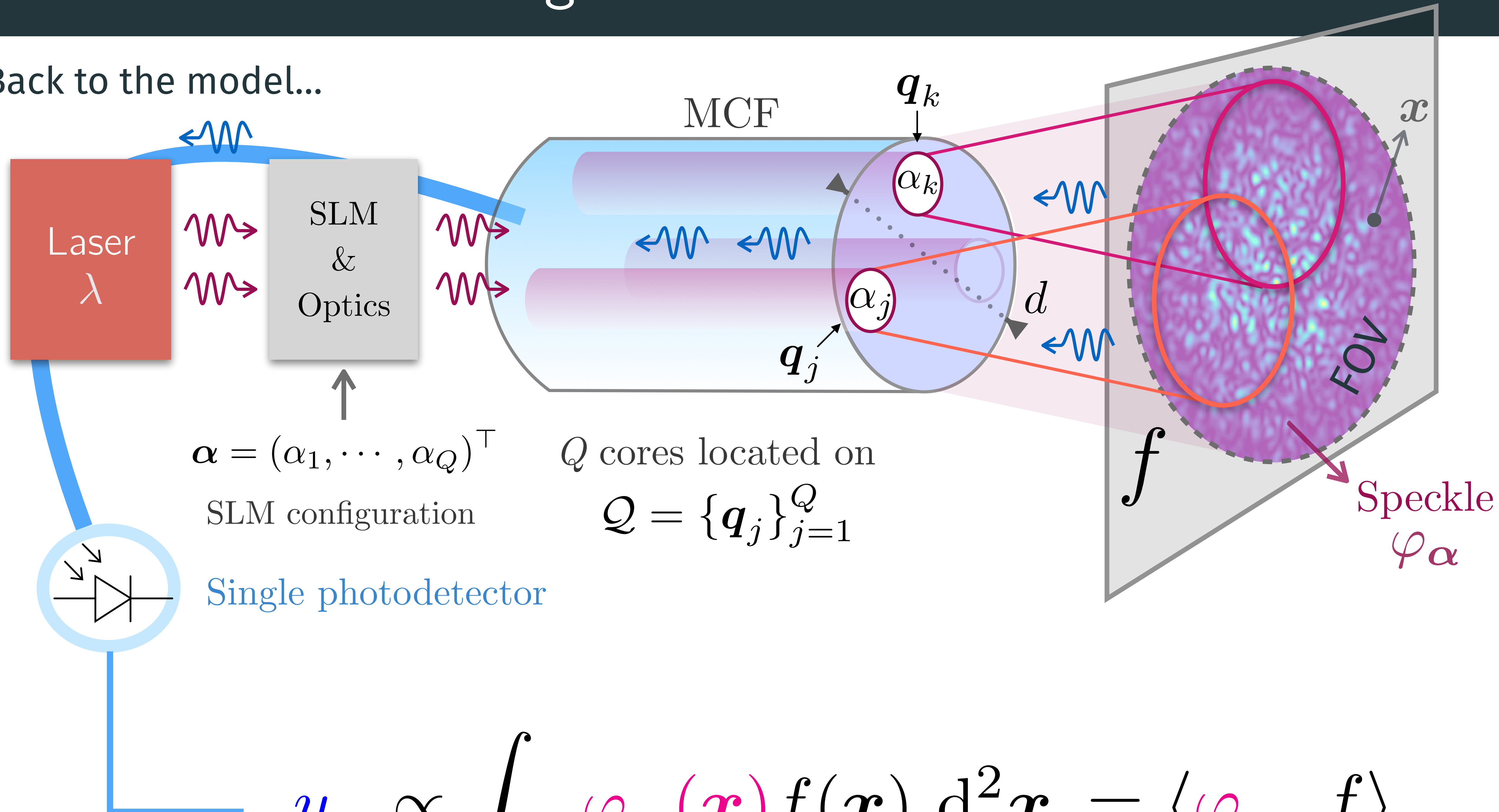

$$y_{\boldsymbol{\alpha}} \propto \int_{\mathbb{R}^2} \varphi_{\boldsymbol{\alpha}}(\boldsymbol{x}) f(\boldsymbol{x}) \, \mathrm{d}^2\boldsymbol{x} = \langle \varphi_{\boldsymbol{\alpha}}, f \rangle$$

Measurement model

Back to the model...

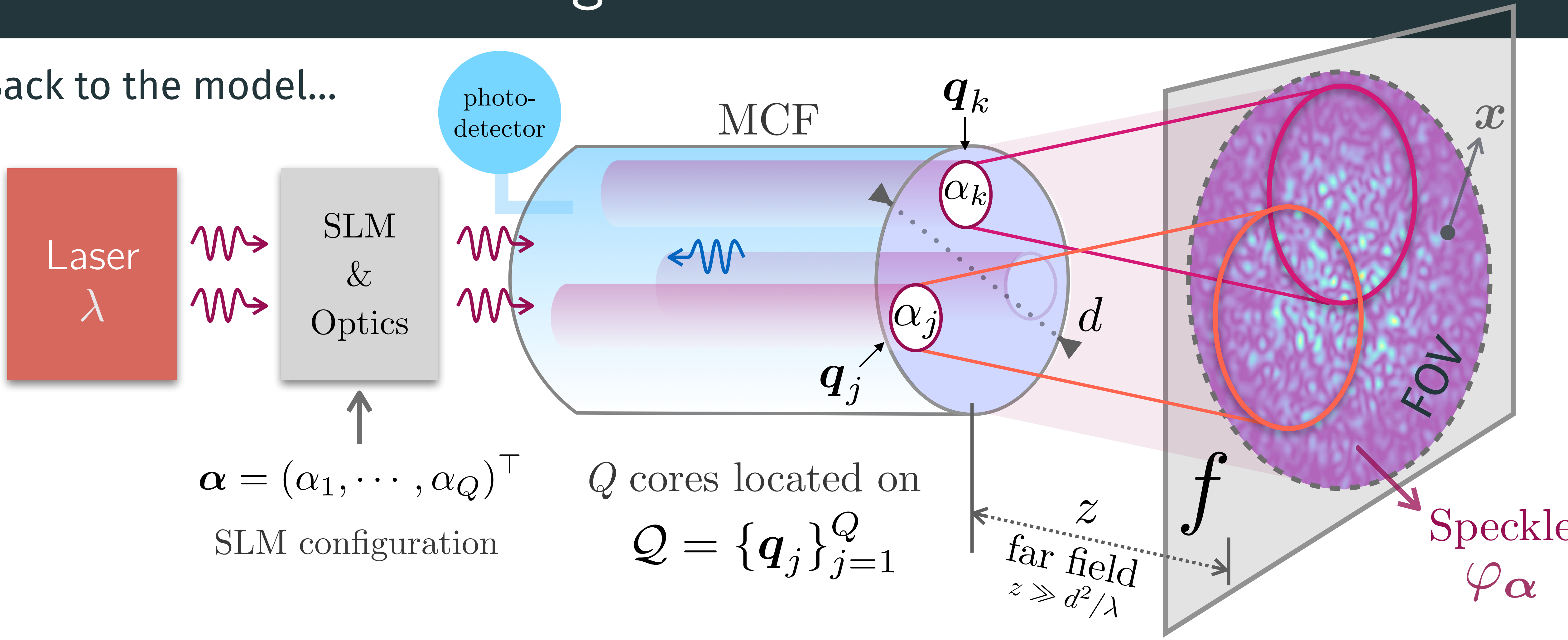

Speckles are interferences: (Under far-field approximation)

$$\varphi_{\boldsymbol{\alpha}}(\boldsymbol{x}) \propto \underbrace{w(\boldsymbol{x})}_{\text{FOV window}} \sum_{j,k=1}^{Q} \alpha_j \alpha_k^* e^{\frac{2\pi \mathrm{i}}{\lambda z}(\boldsymbol{q}_j - \boldsymbol{q}_k)^\top \boldsymbol{x}}$$

Compressive sensing? Gaussian pattern?

(noiseless) Interferometric sensing model

Given $\varphi_{\boldsymbol{\alpha}}(\boldsymbol{x}) = w(\boldsymbol{x}) \sum_{j,k=1}^{Q} \alpha_j \alpha_k^* e^{\frac{2\pi \mathrm{i}}{\lambda z}(\boldsymbol{q}_j - \boldsymbol{q}_k)^\top \boldsymbol{x}}$, we get

$$\langle \varphi_{\boldsymbol{\alpha}}, f \rangle = \sum_{j,k=1}^{Q} \alpha_j \alpha_k^* \left[\int_{\mathbb{R}^2} e^{\frac{2\pi \mathrm{i}}{\lambda z}(\boldsymbol{q}_j - \boldsymbol{q}_k)^\top \boldsymbol{x}} w(\boldsymbol{x}) f(\boldsymbol{x}) \mathrm{d}\boldsymbol{x} \right]$$

(noiseless) Interferometric sensing model

Given $\varphi_{\boldsymbol{\alpha}}(\boldsymbol{x}) = w(\boldsymbol{x}) \sum_{j,k=1}^{Q} \alpha_j \alpha_k^* e^{\frac{2\pi \mathrm{i}}{\lambda z}(\boldsymbol{q}_j - \boldsymbol{q}_k)^\top \boldsymbol{x}}$, we get

$$\langle \varphi_{\boldsymbol{\alpha}}, f \rangle = \sum_{j,k=1}^{Q} \alpha_j \alpha_k^* \left[\int_{\mathbb{R}^2} e^{\frac{2\pi \mathrm{i}}{\lambda z}(\boldsymbol{q}_j - \boldsymbol{q}_k)^\top \boldsymbol{x}} w(\boldsymbol{x}) f(\boldsymbol{x}) \mathrm{d}\boldsymbol{x} \right]$$

$$\to \boldsymbol{\alpha}^* \boldsymbol{\mathcal{I}}[wf]\, \boldsymbol{\alpha}$$ → ROP!!

with the (Hermitian) *interferometric matrix* $\boldsymbol{\mathcal{I}}[wf] \in \mathbb{C}^{Q \times Q}$ s.t.

$$(\boldsymbol{\mathcal{I}}[wf])_{j,k} := \int_{\mathbb{R}^2} e^{\frac{2\pi \mathrm{i}}{\lambda z}(\boldsymbol{q}_j - \boldsymbol{q}_k)^\top \boldsymbol{x}}\, w(\boldsymbol{x}) f(\boldsymbol{x})\, \mathrm{d}\boldsymbol{x}.$$

(noiseless) Interferometric sensing model

Given $\varphi_{\boldsymbol{\alpha}}(\boldsymbol{x}) = w(\boldsymbol{x}) \sum_{j,k=1}^{Q} \alpha_j \alpha_k^* e^{\frac{2\pi \mathrm{i}}{\lambda z}(\boldsymbol{q}_j - \boldsymbol{q}_k)^\top \boldsymbol{x}}$, we get

$$\langle \varphi_{\boldsymbol{\alpha}}, f\rangle = \sum_{j,k=1}^{Q} \alpha_j \alpha_k^* \left[\int_{\mathbb{R}^2} e^{\frac{2\pi \mathrm{i}}{\lambda z}(\boldsymbol{q}_j - \boldsymbol{q}_k)^\top \boldsymbol{x}} w(\boldsymbol{x}) f(\boldsymbol{x}) \mathrm{d}\boldsymbol{x} \right]$$

$$\rightarrow \boldsymbol{\alpha}^* \boldsymbol{\mathcal{I}}[wf]\, \boldsymbol{\alpha} \quad \rightarrow \text{ROP!!}$$

with the (Hermitian) *interferometric matrix* $\boldsymbol{\mathcal{I}}[wf] \in \mathbb{C}^{Q\times Q}$ s.t.

$$(\boldsymbol{\mathcal{I}}[wf])_{j,k} := \int_{\mathbb{R}^2} e^{\underbrace{\frac{2\pi \mathrm{i}}{\lambda z}(\boldsymbol{q}_j - \boldsymbol{q}_k)}_{\boldsymbol{u}}{}^\top \boldsymbol{x}}\, w(\boldsymbol{x}) f(\boldsymbol{x})\, \mathrm{d}\boldsymbol{x}.$$

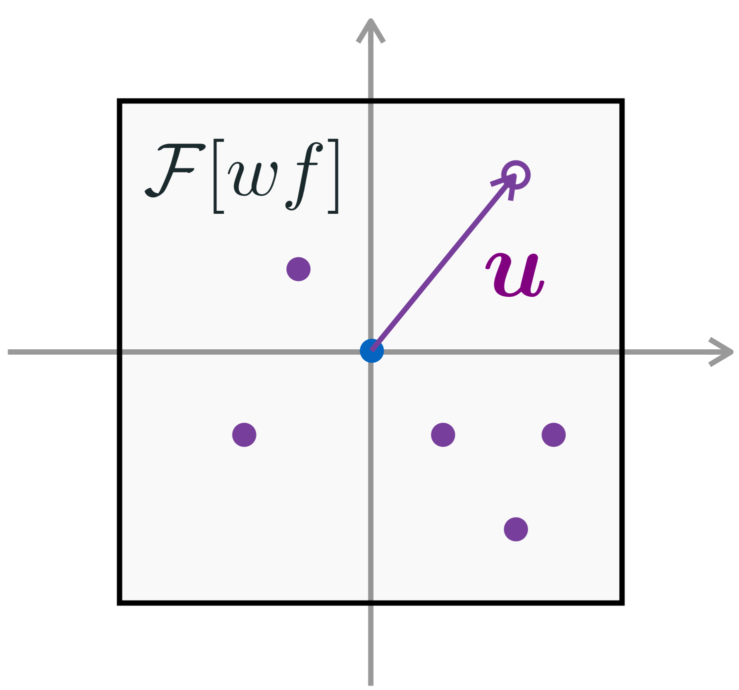

$\boldsymbol{u} \in \mathcal{V} := \frac{1}{\lambda z}(\mathcal{Q} - \mathcal{Q})$

Observation 1: denser Fourier sampling if

$$|\mathcal{V}| \simeq Q^2$$

- Lattices are bad core arrangements
- Fermat's spiral is not bad

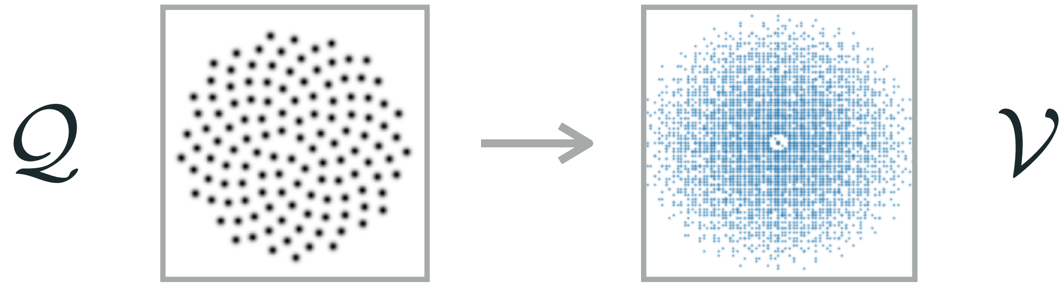

(noiseless) Interferometric sensing model

Given $\varphi_{\boldsymbol{\alpha}}(\boldsymbol{x}) = w(\boldsymbol{x}) \sum_{j,k=1}^{Q} \alpha_j \alpha_k^* e^{\frac{2\pi \mathrm{i}}{\lambda z}(\boldsymbol{q}_j - \boldsymbol{q}_k)^\top \boldsymbol{x}}$, we get

$$\langle \varphi_{\boldsymbol{\alpha}}, f \rangle = \sum_{j,k=1}^{Q} \alpha_j \alpha_k^* \Big[\int_{\mathbb{R}^2} e^{\frac{2\pi \mathrm{i}}{\lambda z}(\boldsymbol{q}_j - \boldsymbol{q}_k)^\top \boldsymbol{x}} w(\boldsymbol{x}) f(\boldsymbol{x}) \mathrm{d}\boldsymbol{x} \Big]$$

$$\to \boldsymbol{\alpha}^* \boldsymbol{\mathcal{I}}[wf] \, \boldsymbol{\alpha}$$ → ROP!!

with the (Hermitian) *interferometric matrix* $\boldsymbol{\mathcal{I}}[wf] \in \mathbb{C}^{Q \times Q}$ s.t.

$$(\boldsymbol{\mathcal{I}}[wf])_{j,k} := \int_{\mathbb{R}^2} e^{\underbrace{\frac{2\pi \mathrm{i}}{\lambda z}(\boldsymbol{q}_j - \boldsymbol{q}_k)^\top}_{\boldsymbol{u}} \boldsymbol{x}} \, w(\boldsymbol{x}) f(\boldsymbol{x}) \, \mathrm{d}\boldsymbol{x}.$$

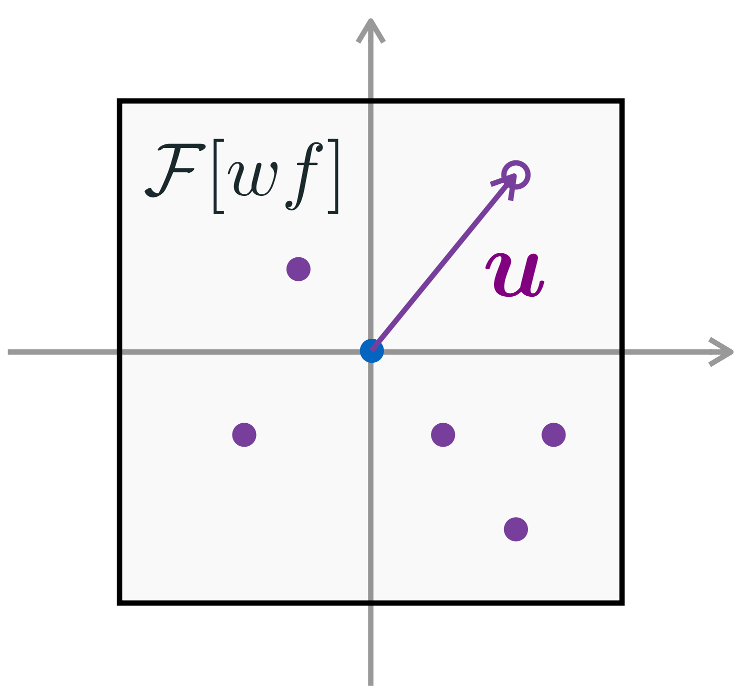

$\boldsymbol{u} \in \mathcal{V} := \frac{1}{\lambda z}(\mathcal{Q} - \mathcal{Q})$

Observation 2:

Low-complexity on f
→
Low-complexity on $\boldsymbol{\mathcal{I}}$.

e.g., sparsity → low-rank

(noiseless) Interferometric sensing model

Given $\varphi_{\boldsymbol{\alpha}}(\boldsymbol{x}) = w(\boldsymbol{x}) \sum_{j,k=1}^{Q} \alpha_j \alpha_k^* e^{\frac{2\pi \mathrm{i}}{\lambda z}(\boldsymbol{q}_j - \boldsymbol{q}_k)^\top \boldsymbol{x}}$, we get

$$\langle \varphi_{\boldsymbol{\alpha}}, f \rangle = \sum_{j,k=1}^{Q} \alpha_j \alpha_k^* \left[\int_{\mathbb{R}^2} e^{\frac{2\pi \mathrm{i}}{\lambda z}(\boldsymbol{q}_j - \boldsymbol{q}_k)^\top \boldsymbol{x}} w(\boldsymbol{x}) f(\boldsymbol{x}) \mathrm{d}\boldsymbol{x} \right]$$

$$\dashrightarrow \boldsymbol{\alpha}^* \, \boldsymbol{\mathcal{I}}[wf] \, \boldsymbol{\alpha} \quad \to \text{ROP!!}$$

with the (Hermitian) *interferometric matrix* $\boldsymbol{\mathcal{I}}[wf] \in \mathbb{C}^{Q \times Q}$ s.t.

$$(\boldsymbol{\mathcal{I}}[wf])_{j,k} := \int_{\mathbb{R}^2} e^{\underbrace{\frac{2\pi \mathrm{i}}{\lambda z}(\boldsymbol{q}_j - \boldsymbol{q}_k)}_{\boldsymbol{u}}{}^\top \boldsymbol{x}} \, w(\boldsymbol{x}) f(\boldsymbol{x}) \, \mathrm{d}\boldsymbol{x}.$$

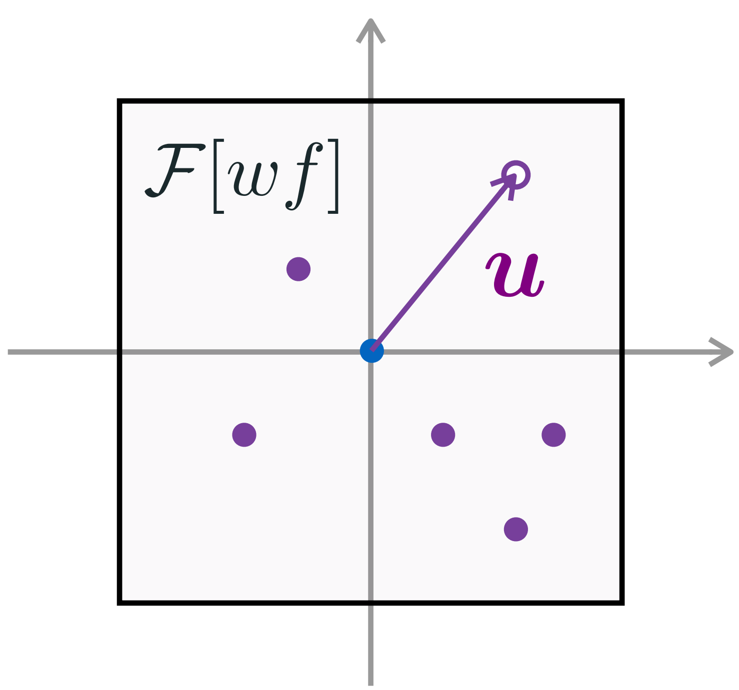

$$\boldsymbol{u} \in \mathcal{V} := \tfrac{1}{\lambda z}(\mathcal{Q} - \mathcal{Q})$$

Observation 3: Similarity with radioastronomy!

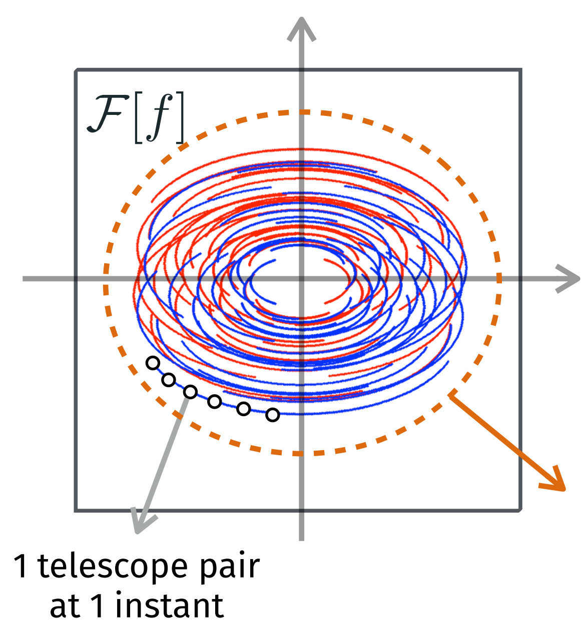

Interferometric sensing model

Composition of two sensing methods

$Q \times Q$ ①

$$\boldsymbol{y} = (y_{\boldsymbol{\alpha}_1}, \cdots, y_{\boldsymbol{\alpha}_m})^\top = \mathcal{A}(\boldsymbol{\mathcal{I}}[wf]) + \text{noise},$$

② $m \times Q^2$

with $\mathcal{A}(\boldsymbol{M}) := \{\langle \boldsymbol{\alpha}_j \boldsymbol{\alpha}_j^*, \boldsymbol{M} \rangle_{\mathrm{F}}\}_{j=1}^m$.

Sample complexities of interest:

② Does $\mathcal{A}$ capture enough from $\boldsymbol{\mathcal{I}}$? $\leftrightarrow$ m big enough?

① Does $\boldsymbol{\mathcal{I}}$ capture enough from f? $\leftrightarrow$ Q big enough?

Core arrangement?

A few answers from a few simplifications ...

Theory + Simulations + Experimental results

ROP debiasing

Stabilization of the ROP operator $\rightarrow$ *debiasing*

$$\boldsymbol{\mathcal{A}}^{\mathrm{c}} : \boldsymbol{\mathcal{J}} \in \mathcal{H}^{Q} \mapsto \big(\langle \boldsymbol{A}^{\mathrm{c}}_{m}, \boldsymbol{\mathcal{J}} \rangle\big)_{m=1}^{M} \in \mathbb{R}^{M},$$

with $\boldsymbol{A}^{\mathrm{c}}_{m} := \boldsymbol{\alpha}_{m}\boldsymbol{\alpha}^{*}_{m} - \frac{1}{M}\sum_{j=1}^{M} \boldsymbol{\alpha}_{j}\boldsymbol{\alpha}^{*}_{j}$

Equivalence: centering the measurement $\equiv$ debiasing the ROP operator

Given $\boldsymbol{y} = \boldsymbol{\mathcal{A}}(\boldsymbol{\mathcal{J}})$,

$$\underbrace{y^{\mathrm{c}}_{k} := y_{k} - \frac{1}{M}\sum_{j=1}^{M} y_{j}}_{\text{centering}} \text{ for } k \in [M] \Rightarrow \boldsymbol{y}^{\mathrm{c}} = \boldsymbol{\mathcal{A}}^{\mathrm{c}}(\boldsymbol{\mathcal{J}}).$$

Theoretical guarantees: Proposed reconstruction

$$\tilde{\boldsymbol{f}} = \arg\min_{\boldsymbol{v}\in\mathbb{R}^N} \|\boldsymbol{v}\|_1 \text{ s.t. } \Big\|\boldsymbol{y}^{\mathrm{c}} - \underbrace{\varpi\, \boldsymbol{\mathcal{A}}^{\mathrm{c}}\big(\mathcal{R}(\boldsymbol{\Phi}\boldsymbol{v})\big)}_{=:\boldsymbol{\mathcal{B}}(\boldsymbol{v})}\Big\|_1 \leq \epsilon$$

Theoretical guarantees: Proposed reconstruction

$$\tilde{\boldsymbol{f}} = \arg\min_{\boldsymbol{v}\in\mathbb{R}^N} \|\boldsymbol{v}\|_1 \text{ s.t. } \big\|\boldsymbol{y}^{\mathrm{c}} - \underbrace{\varpi\,\boldsymbol{\mathcal{A}}^{\mathrm{c}}\big(\mathcal{R}(\boldsymbol{\Phi v})\big)}_{=:\boldsymbol{\mathcal{B}}(\boldsymbol{v})}\big\|_1 \leq \epsilon$$

Under certain conditions, if

$$M \geqslant C K \ln(\tfrac{12eN}{K}) \text{ and } Q(Q-1) \geqslant 4K \,\mathrm{plog}(N, K, \delta),$$

$\exists 0 < \mathsf{m}_K < \mathsf{M}_K$ such that, w.h.p,

$$\mathsf{m}_K\|\boldsymbol{v}\| \leqslant \tfrac{1}{M}\|\boldsymbol{\mathcal{B}}(\boldsymbol{v})\|_1 \leqslant \mathsf{M}_K\|\boldsymbol{v}\|, \quad \forall \boldsymbol{v} \in \Sigma_K.$$

$\mathrm{RIP}_{\ell_2/\ell_1}$

Instance optimality:

Provided $\boldsymbol{\mathcal{B}}$ has the $\mathrm{RIP}_{\ell_2/\ell_1}(K', \mathsf{m}'_K, \mathsf{M}'_K)$, for $K' = O(K)$, $\exists C_0, D_0 > 0$,

$$\|\boldsymbol{f} - \tilde{\boldsymbol{f}}\| \leq C_0 \frac{\|\boldsymbol{f} - \boldsymbol{f}_K\|_1}{\sqrt{K}} + D_0 \frac{\epsilon}{M}.$$

1-D simulations: phase transition diagrams

Simplified setting:

1-D core arrangement, $N = 256$

K-sparse vectors

Random $\{\boldsymbol{\alpha}_j\}_{j=1}^{M}$

Q, M, K varying

80 trials, Success if $\geq$ 40 dB

Simplified setting:

- 1-D core arrangement, $N = 256$
- K-sparse vectors
- Random $\{\boldsymbol{\alpha}_j\}_{j=1}^{M}$
- Q, M, K varying
- 80 trials, Success if $\geq$ 40 dB

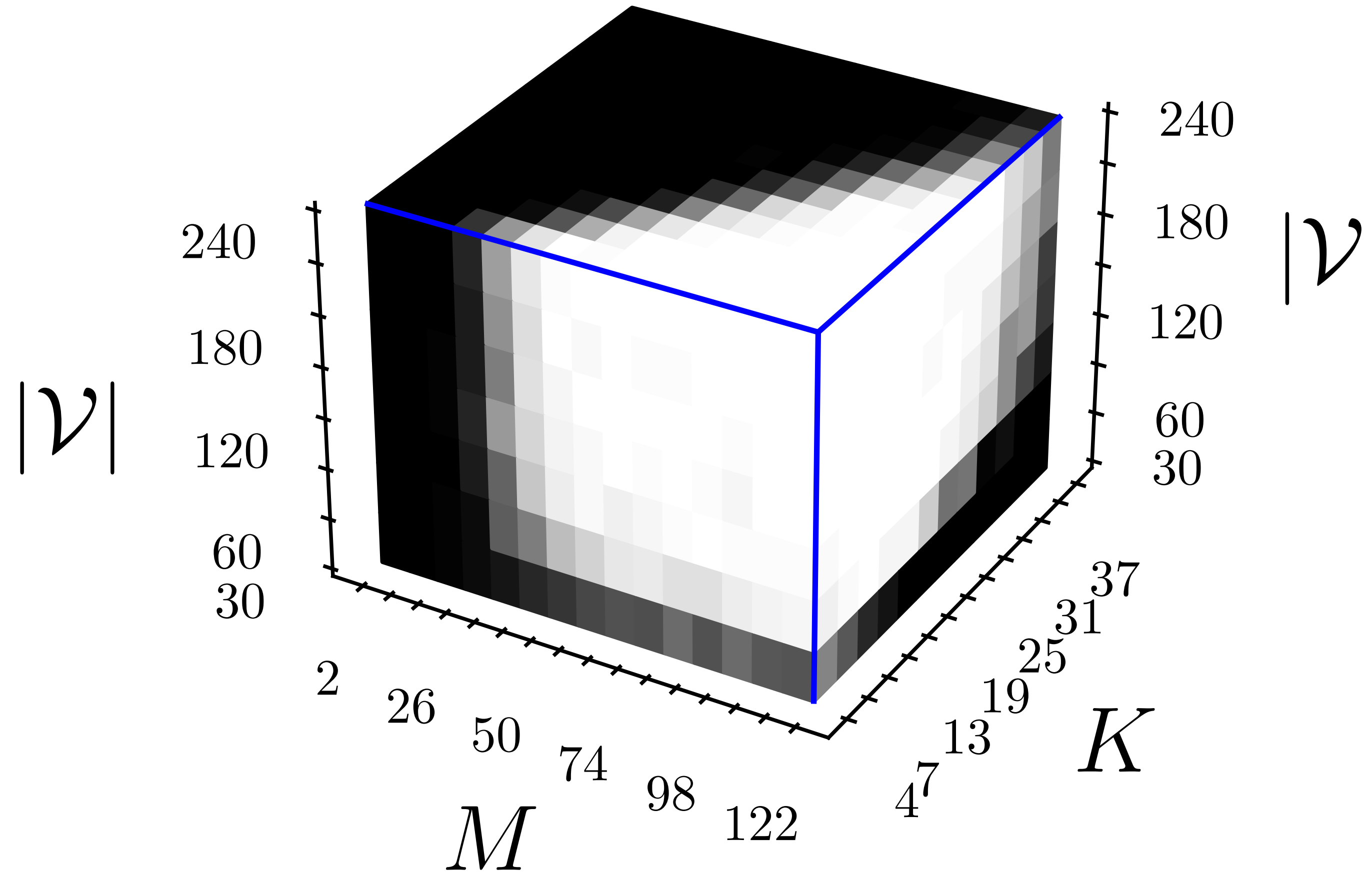

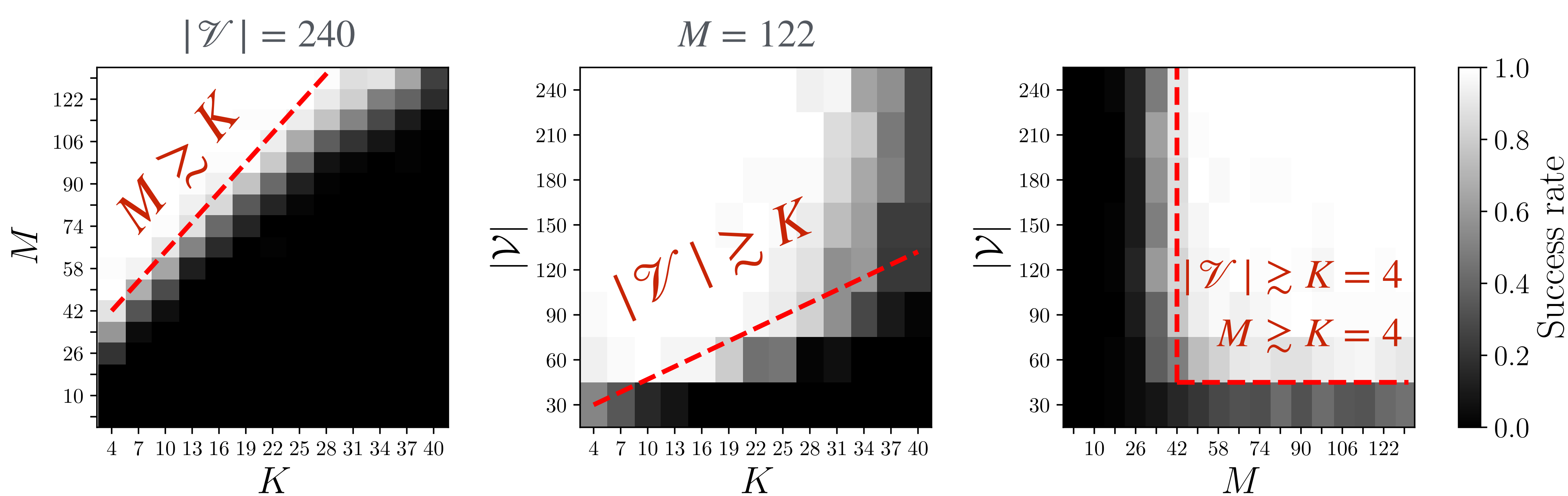

Experiments (in Institut Fresnel, France)

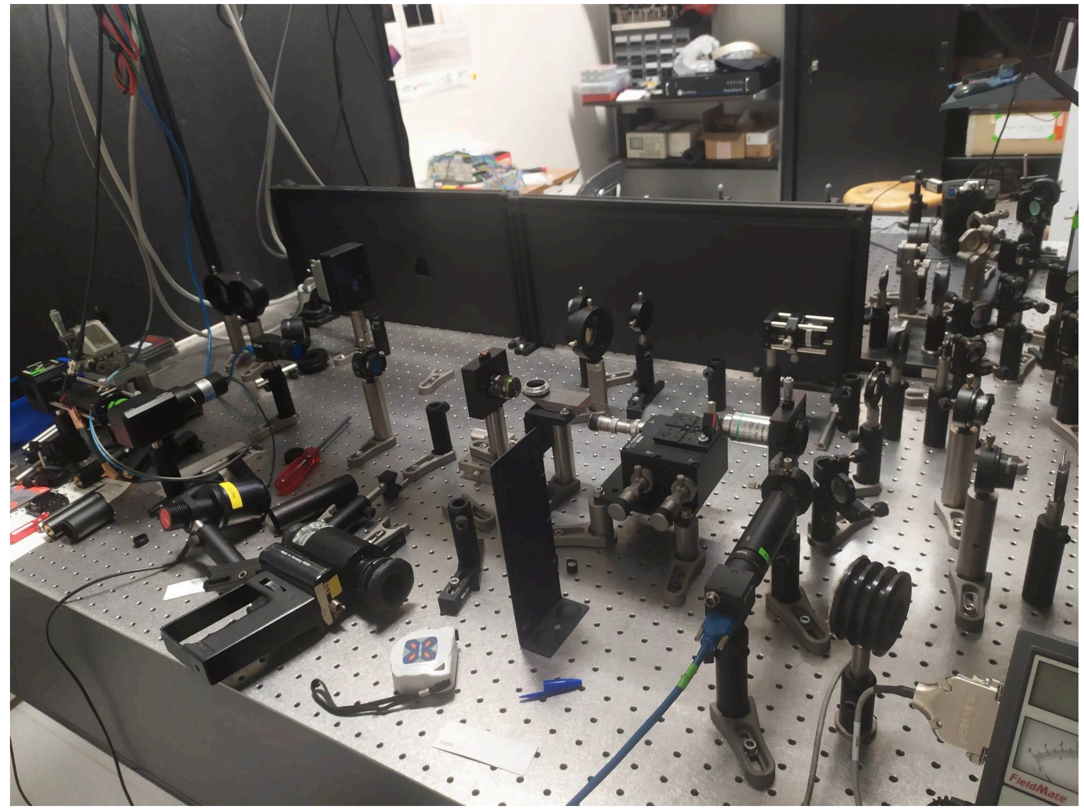

Single pixel
=
Pixel summation

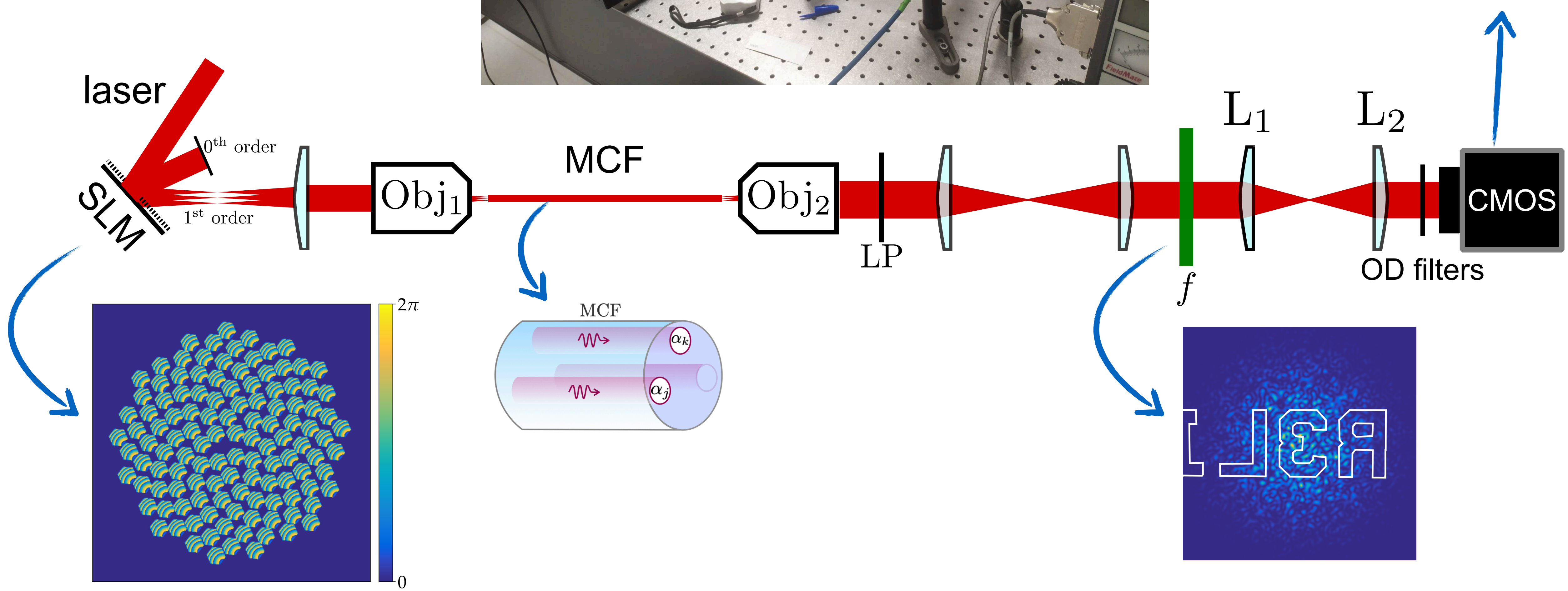

Experiments (in Institut Fresnel, France)

Special points of attention:

- MCF must be calibrated
- MCF system in transmission mode
- Speckle calibration (system imperfections)

  e.g., $\neq$ core radius, locations, ...

(Adapted from xkcd #1233)

Reconstruction method: TV regularizer

$$\tilde{\boldsymbol{f}} = \arg\min_{\boldsymbol{f}} \; \tfrac{1}{2}\|\boldsymbol{y}^{\mathrm{c}} - \boldsymbol{\mathcal{B}}(\boldsymbol{f})\|_2^2 + \rho\|\boldsymbol{f}\|_{\mathrm{TV}} \text{ s.t. } \boldsymbol{f} \geq 0,$$

ROP + interfero

Set empirically

Experiments (in Institut Fresnel, France)

Average SNR (5 trials)

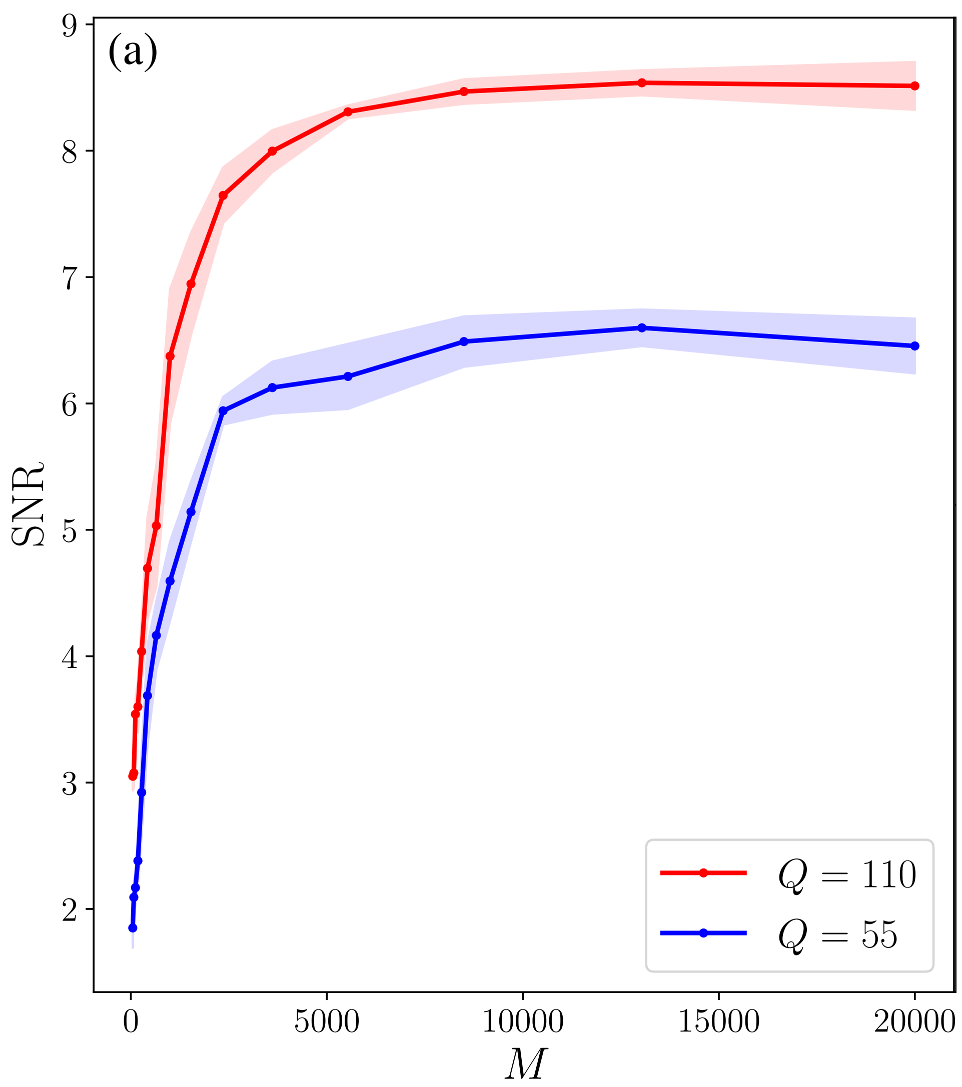

USAF target $Q = 55$ $Q = 110$

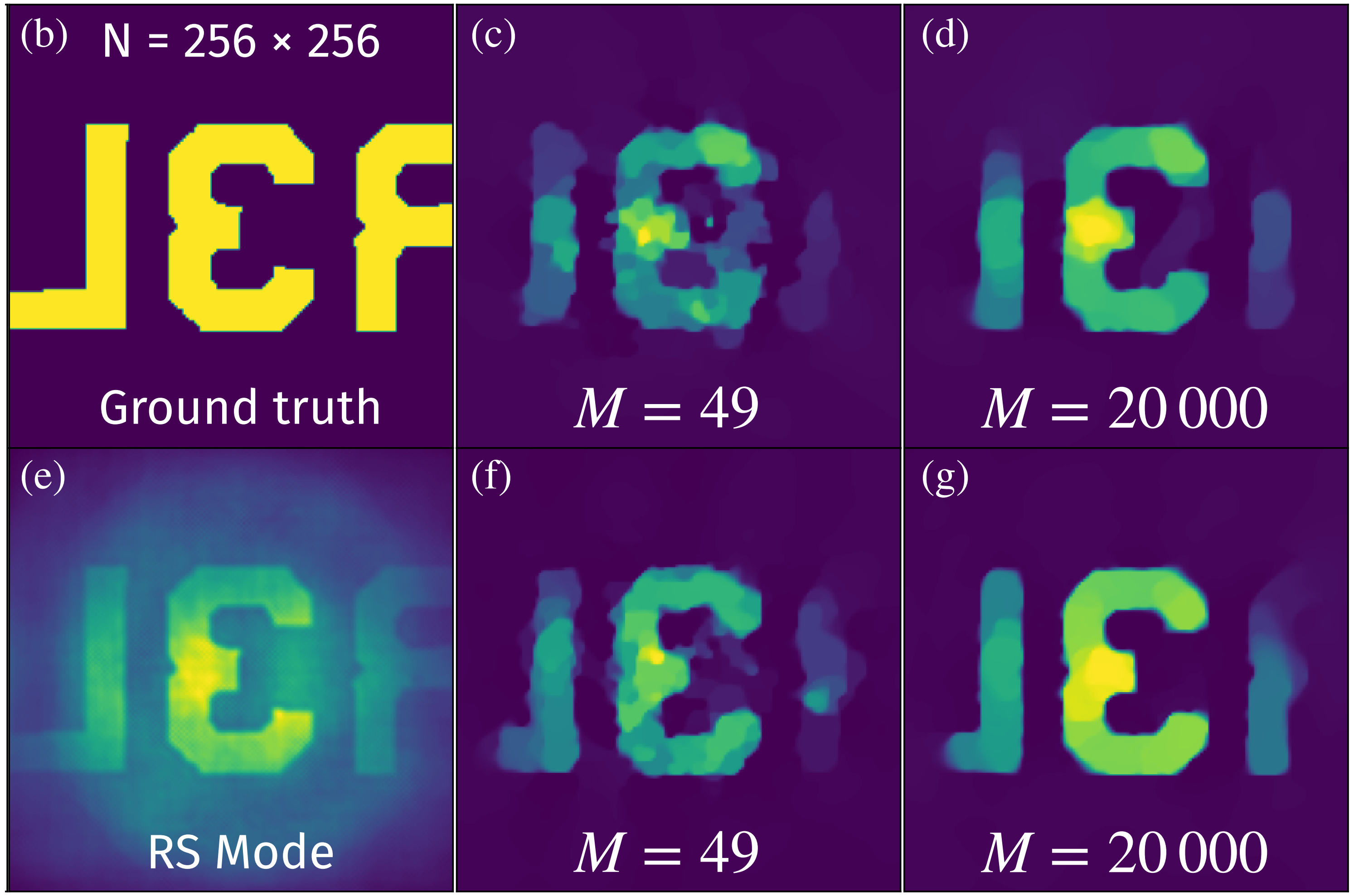

Optical sketching & ROP

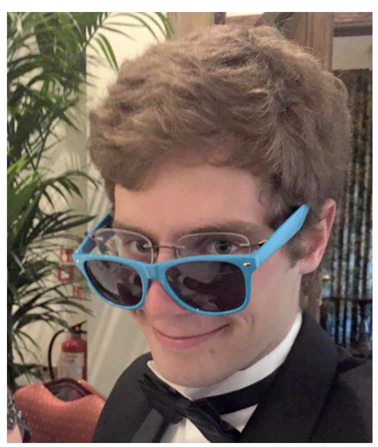

R. Delogne[*]

V. Schellekens[°]

L. Daudet[+]

L. Jacques[*]

*: ISPGroup, INMA, UCLouvain, Belgium. †: Institut Fresnel, France.

°: imec, Belgium. +: LightOn, France.

Sketching with an Optical Processing Unit

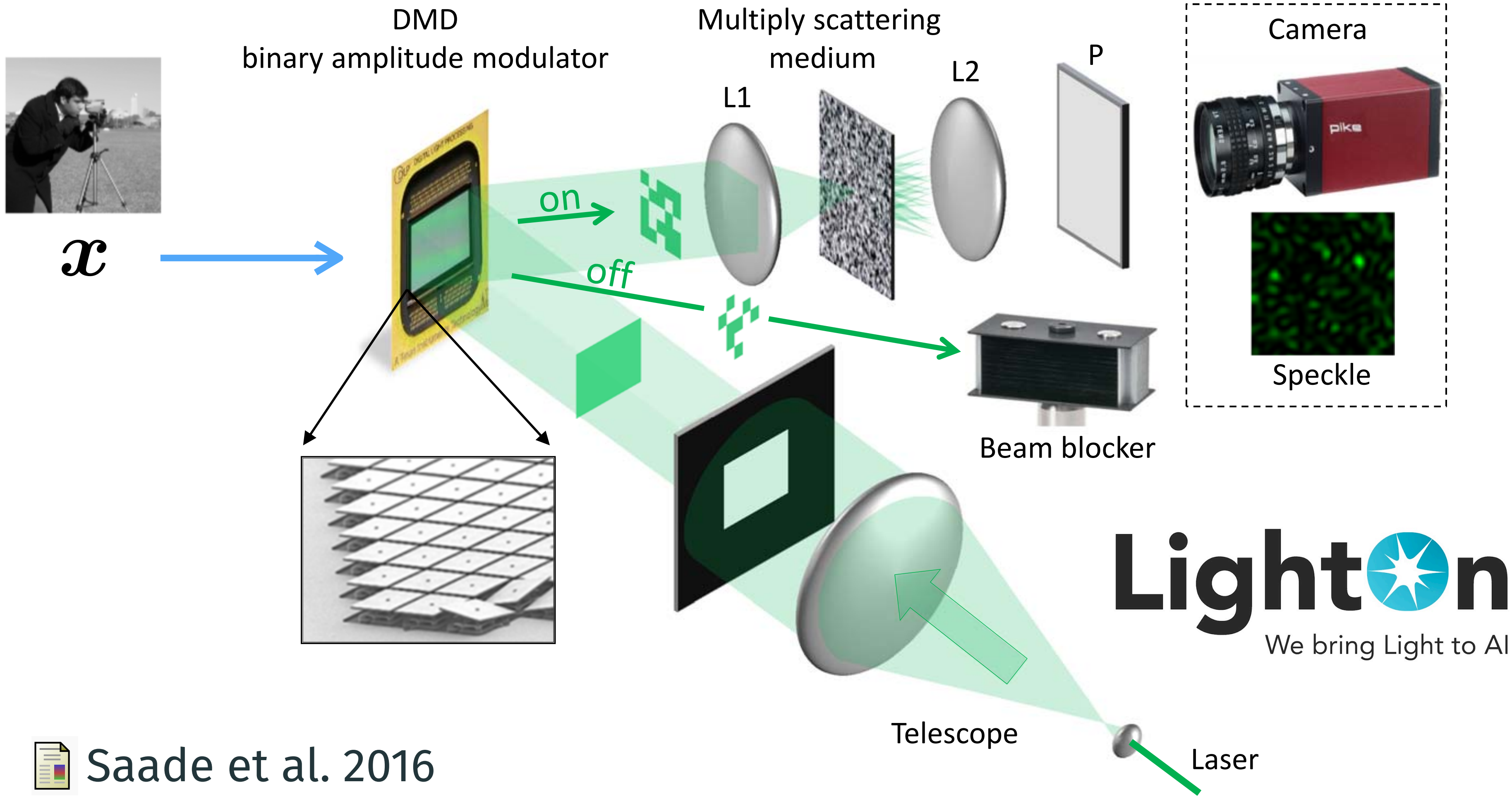

Saade et al. 2016

Device to collect
random feature vectors
"at the speed of light"

$y(x)$

Sketch

Machine Learning

Sketching with an Optical Processing Unit

$\boldsymbol{x}$ →

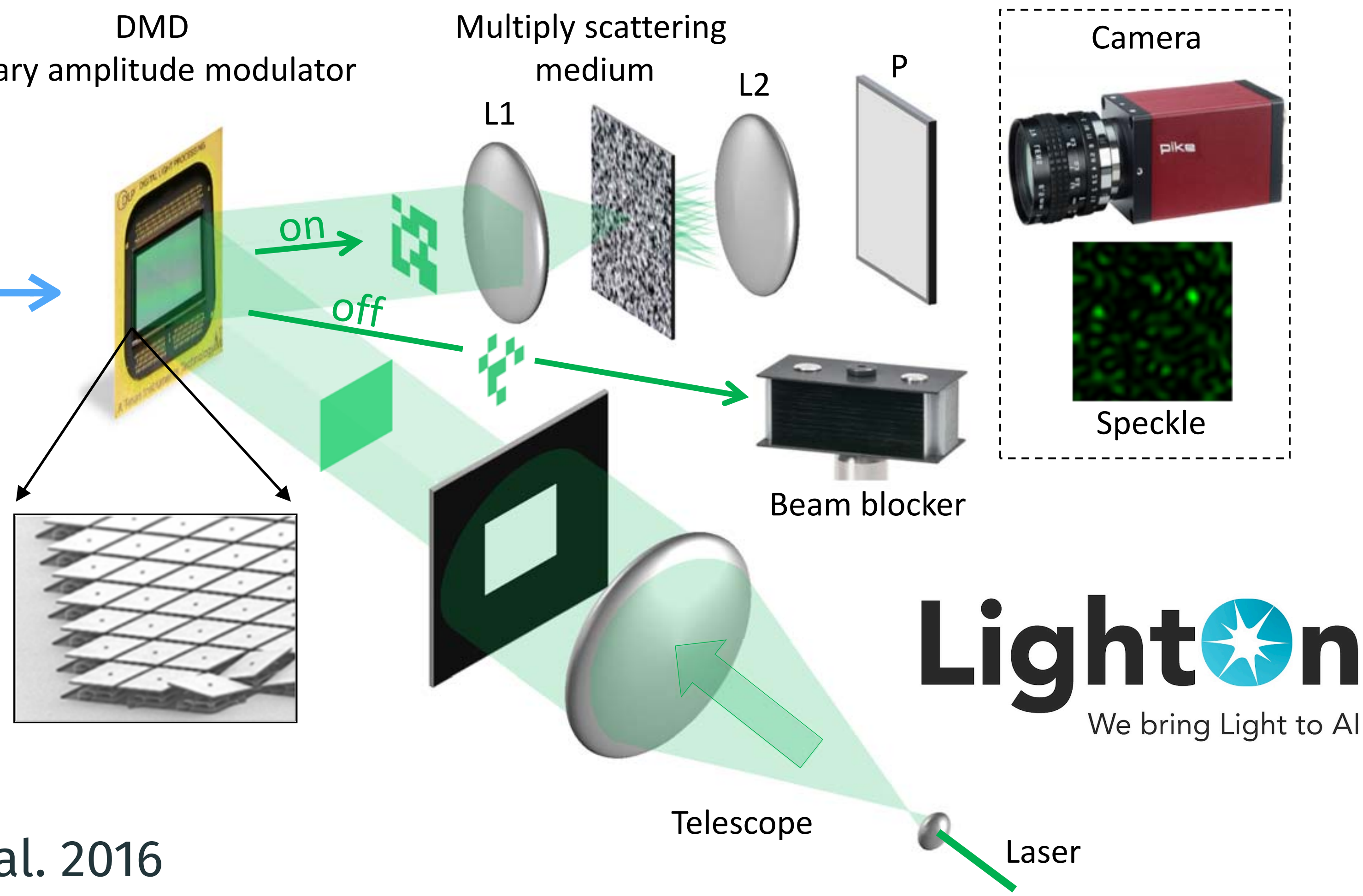

Saade et al. 2016

→ Device to collect
random feature vectors
"at the speed of light"

$\boldsymbol{y}(\boldsymbol{x})$

Sketch

↓

Machine Learning

Implicit random rank-one projection model: (with m pixels)

$$\boldsymbol{y} = \left(|\langle \boldsymbol{a}_i, \boldsymbol{x}\rangle|^2\right)_{i=1}^{m} = \left(\langle \boldsymbol{a}_i \boldsymbol{a}_i^*, \boldsymbol{x}\boldsymbol{x}^*\rangle_F\right)_{i=1}^{m} = \boldsymbol{\mathcal{A}}(\boldsymbol{x})$$

Complex Gaussian (Stat. Phys.)

Rank-one

OPU operator

General research question

How much information can we (easily*) decode
from the OPU/ROP sketch $\boldsymbol{\mathcal{A}}$?

*: e.g., linearly

General research question

How much information can we (easily*) decode
from the OPU/ROP sketch $\boldsymbol{\mathcal{A}}$?

For instance,

- Can we extract local information about $\boldsymbol{x}$?
- Or moments? Frequencies?

Applications:

- change point/anomaly detection in data stream, industrial processes, monitoring, ...

*: e.g., linearly

$\boldsymbol{x}$

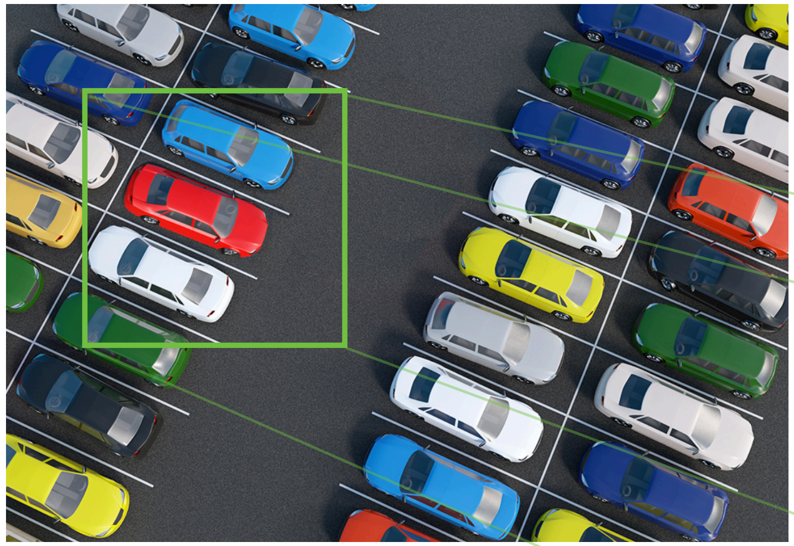

LightOn
We bring Light to AI

$\mathcal{A}(\boldsymbol{x})$

Sketch

$\boldsymbol{x}'$

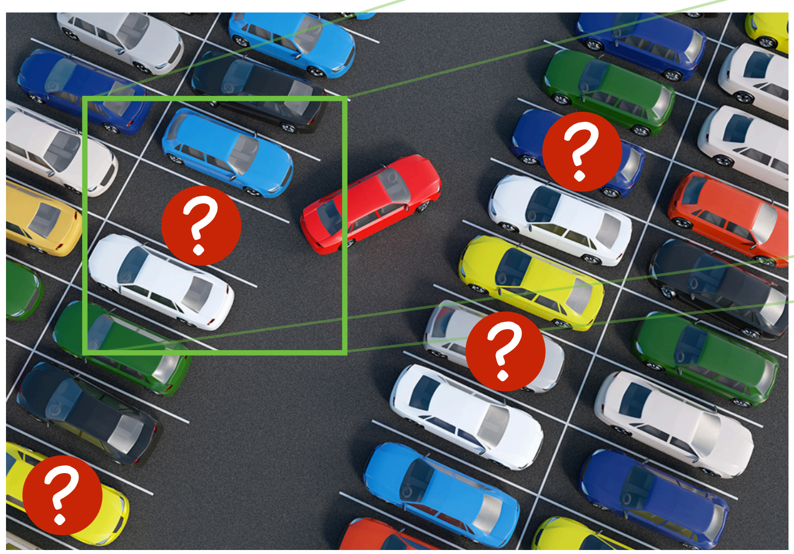

LightOn
We bring Light to AI

$\mathcal{A}(\boldsymbol{x}')$

Sketch

$$\mathcal{A}(\boldsymbol{x}) \text{ or } \mathcal{A}(\boldsymbol{x}') \ ?$$

Estimates of $\langle \boldsymbol{u}, \boldsymbol{x} \rangle$ and $\langle \boldsymbol{u}, \boldsymbol{x}' \rangle$?

$\boldsymbol{u} =$ [1 / 0]

Problem statement, for a general sketching $\boldsymbol{\Psi}$

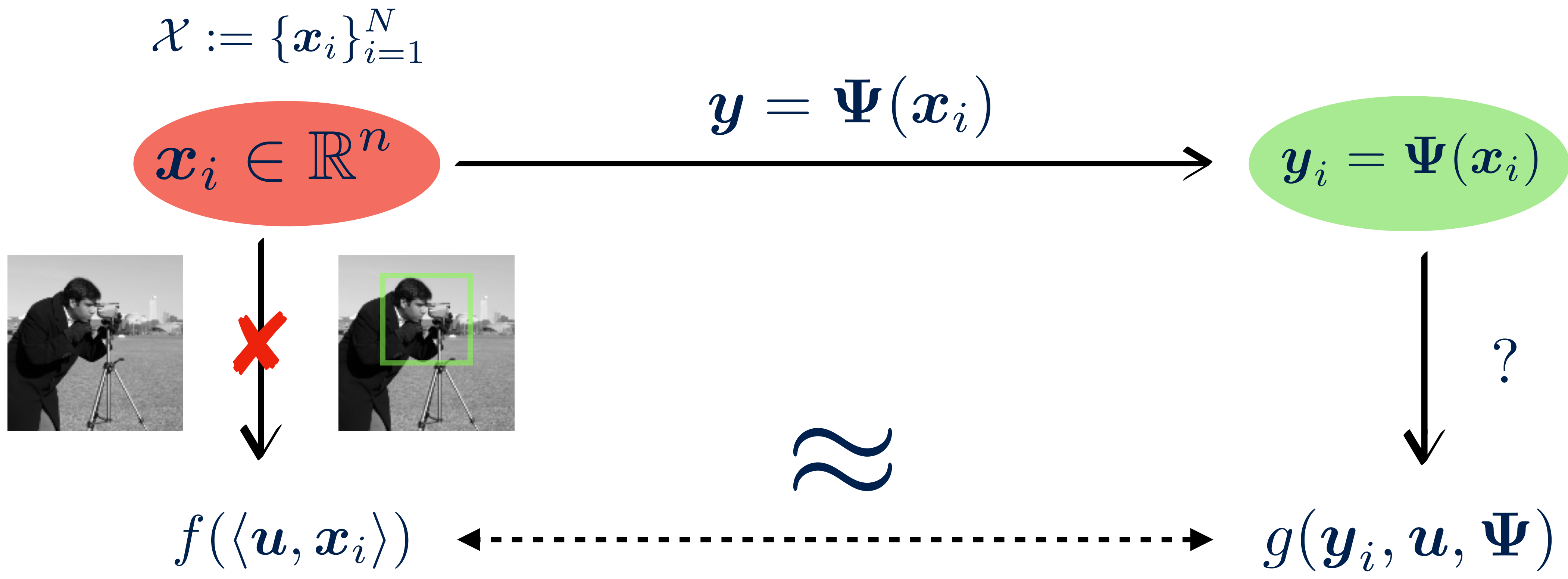

Given $\boldsymbol{\Psi}$, find f and g with $g(\boldsymbol{y}_i, \boldsymbol{u}, \Psi) \approx f(\langle \boldsymbol{u}, \boldsymbol{x}_i \rangle)$?

Problem statement, for a general sketching $\boldsymbol{\Psi}$

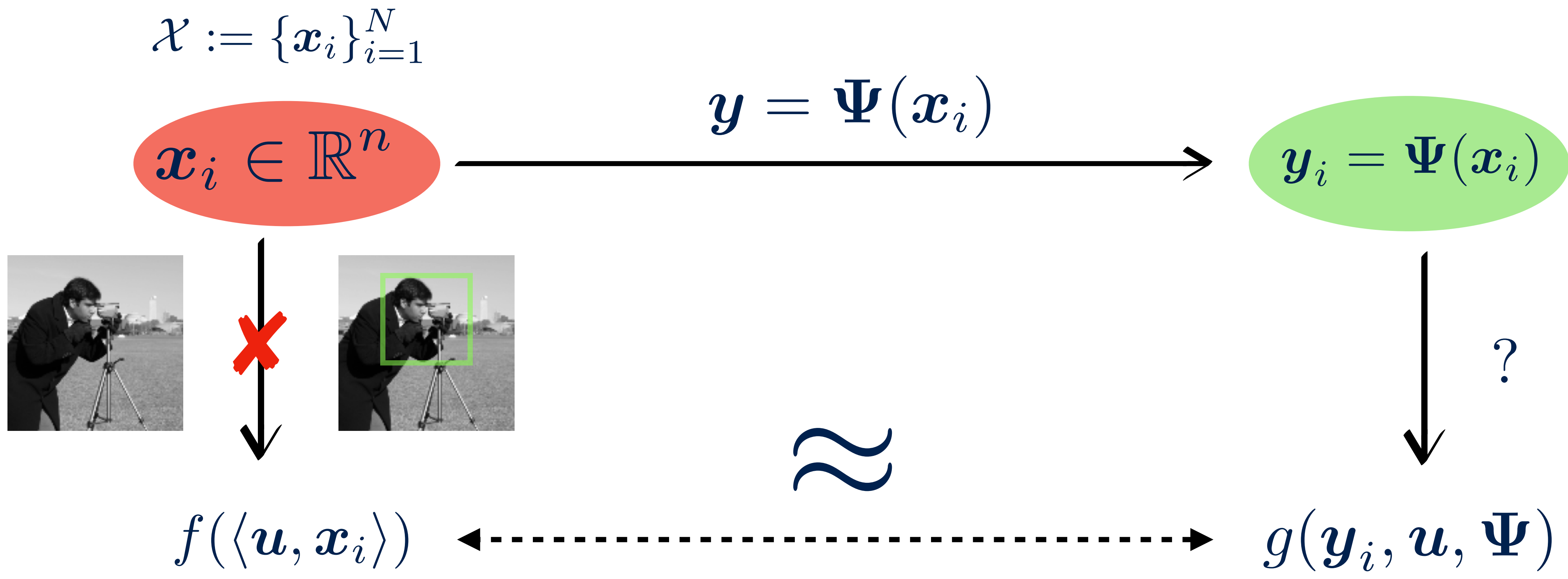

Given $\boldsymbol{\Psi}$, find f and g with $g(\boldsymbol{y}_i, \boldsymbol{u}, \Psi) \approx f(\langle \boldsymbol{u}, \boldsymbol{x}_i \rangle)$?

Answers from classical (linear) compressive sensing: Davenport et al., 2010.

Under certain conditions on $\boldsymbol{\Phi}$ (i.e., RIP):

Sketch comparison; $f = \mathrm{Id}$

$$\boldsymbol{y} = \boldsymbol{\Psi}(\boldsymbol{x}) = \boldsymbol{\Phi x} \ \rightarrow \ g(\boldsymbol{y}, \boldsymbol{u}, \boldsymbol{\Psi}) = \langle \boldsymbol{\Phi u}, \boldsymbol{y} \rangle = \boldsymbol{u}^\top \boldsymbol{\Phi}^\top \boldsymbol{y} \approx \langle \boldsymbol{u}, \boldsymbol{x} \rangle$$

? What are f and g if $\boldsymbol{\Psi} = \mathrm{ROP}$ (i.e., quadratic)?

Let's first debiase the ROP (yet another debiasing)

Debiasing [Chen et al. 2013]

- Quadratic measurements only output strictly positive values
- $\mathbb{E}[\mathcal{A}^{\mathrm{v}}(\boldsymbol{x})] > 0$
- **debiased operator**:

$$\mathcal{B}(\boldsymbol{x}) = \big(\mathcal{A}^{\mathrm{v}}_{2i}(\boldsymbol{x}) - \mathcal{A}^{\mathrm{v}}_{2i+1}(\boldsymbol{x})\big)_{i=1}^{m} \in \mathbb{R}^m,$$

such that $\mathbb{E}[\mathcal{B}(x)] = 0$.

Optically achievable

- If $\boldsymbol{x}$ is binary: $\mathcal{A}^{\mathrm{v}}_{\mathrm{opu}}(\boldsymbol{x}) \approx \mathcal{A}^{\mathrm{v}}(\boldsymbol{x})$
- Time complexity of $\mathcal{O}(1)$.

The Sign Product Embedding (SPE)

Given $\boldsymbol{u} \in \mathbb{R}^n$, with $\|\boldsymbol{u}\| = 1$, and $0 < \delta < 1$, if

$$m \gtrsim \delta^{-2} k \log(n/k\delta),$$

then for all k-sparse signals $\boldsymbol{x} \in \mathbb{R}^n$ in any basis,

$$\left| \tfrac{\pi}{4m} \langle \mathrm{sign}(\mathcal{B}(\boldsymbol{u})), \mathcal{B}(\boldsymbol{x}) \rangle \; - \; \langle \boldsymbol{u}, \boldsymbol{x} \rangle^2 \right| \; \le \; \delta \, \|\boldsymbol{x}\|^2.$$

holds with high probability.

Delogne et al, 2023

$\Rightarrow$ For m large enough,

$$\text{for } \boldsymbol{\Psi} = \boldsymbol{\mathcal{B}} \;\to\; g(\boldsymbol{y}, \boldsymbol{u}, \boldsymbol{\Psi}) = \tfrac{\pi}{4m} \langle \mathrm{sign}\left(\boldsymbol{\mathcal{B}}(\boldsymbol{u})\right), \boldsymbol{y} \rangle \approx \langle \boldsymbol{u}, \boldsymbol{x} \rangle^2$$

Asymmetric sketch comparison

simple projection

$f(\,\cdot\,) = (\,\cdot\,)^2$

Experiments I

Setup

- Sequence of frames $\{\boldsymbol{x}_t\}_{t=0}^{23}$, representing a revolving disk.
- Only access to $\{\boldsymbol{\mathcal{B}}(x_t)\}_{t=0}^{23}$
- **Aim** : Detect the passage of the disk in single quadrants directly in the sketched domain

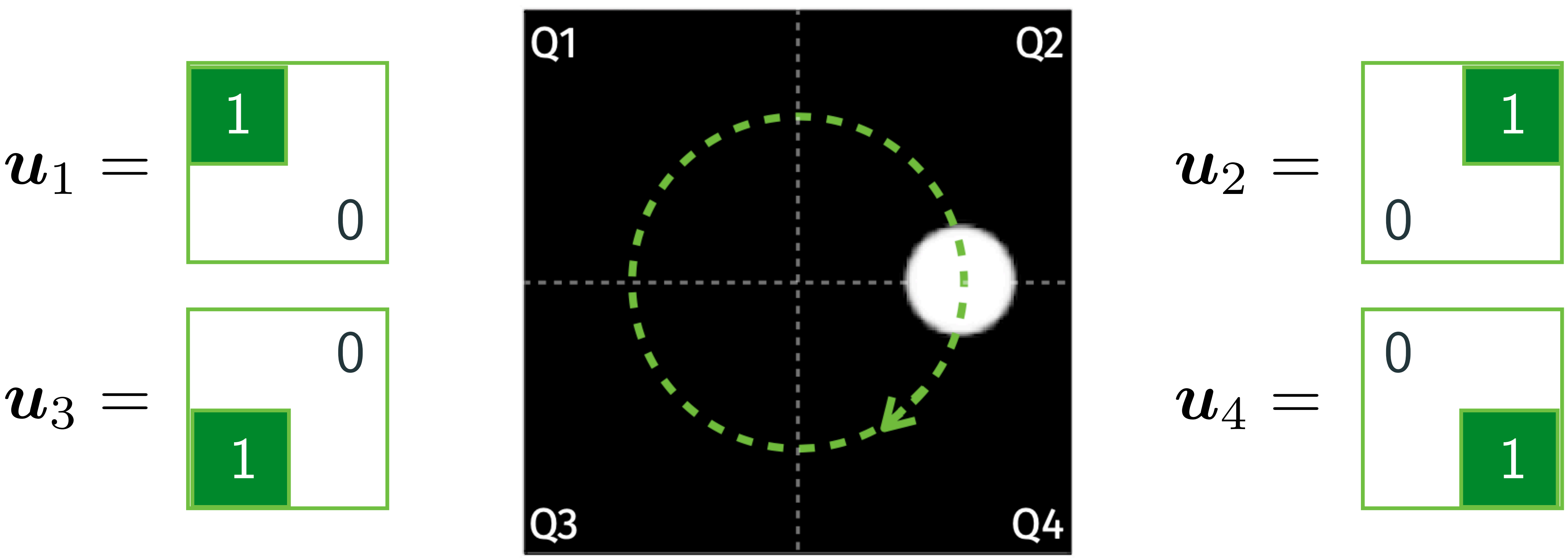

Experiments I

Use the SPE to estimate the *quadrant occupancy*:
$q_j(t) := |\langle \boldsymbol{u}_j, \boldsymbol{x}_t \rangle|^2$ from $\frac{\pi}{4m}\langle \mathrm{sign}(\mathcal{B}_{\mathrm{opu}}(\boldsymbol{u})), \mathcal{B}_{\mathrm{opu}}(\boldsymbol{x}_t) \rangle$

Dashed: $q_j(t)$, continuous: OPU

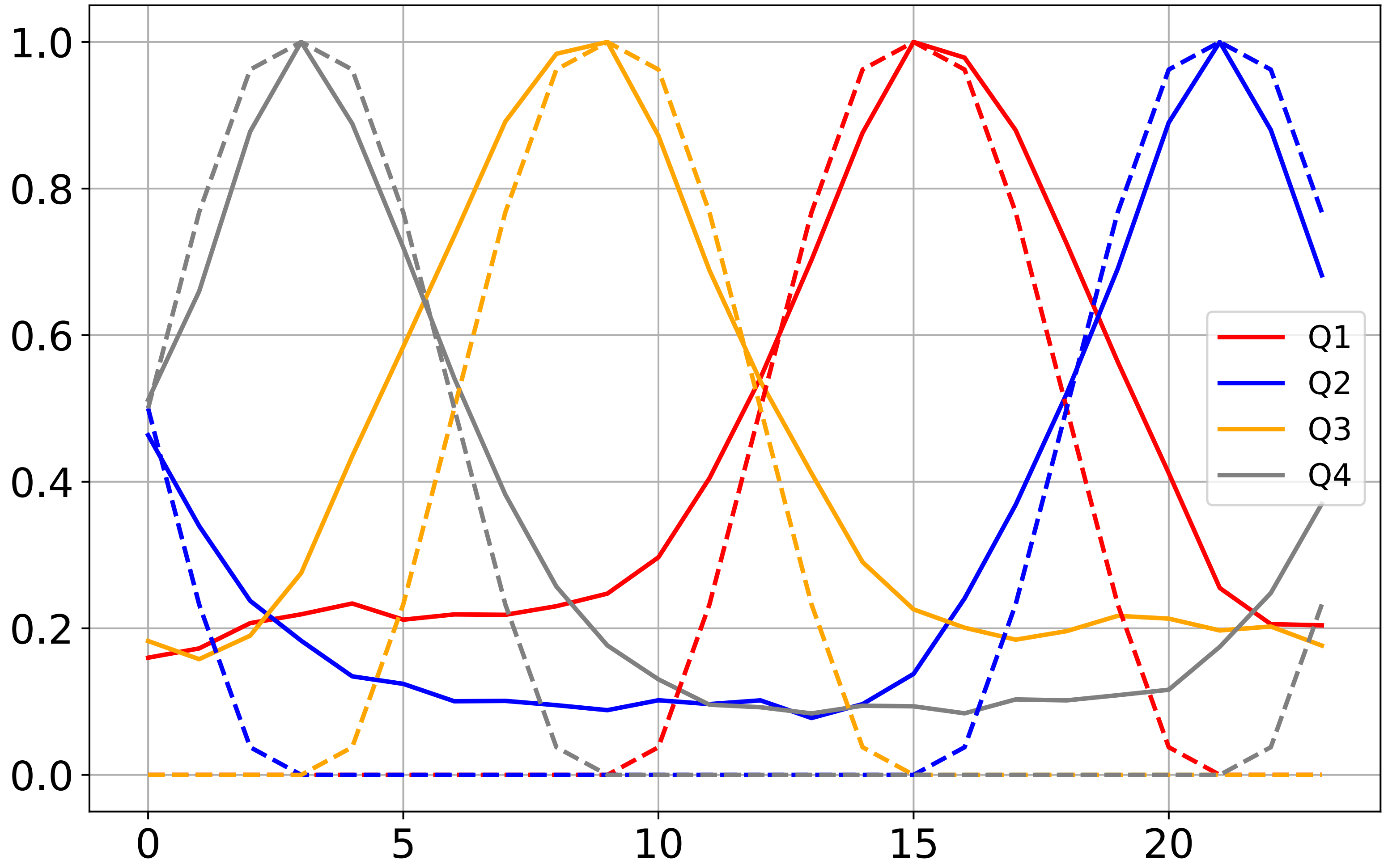

Experiments II

60 000

Training set

10 000

Test set: $\boldsymbol{x}_1, \ldots$

MNIST

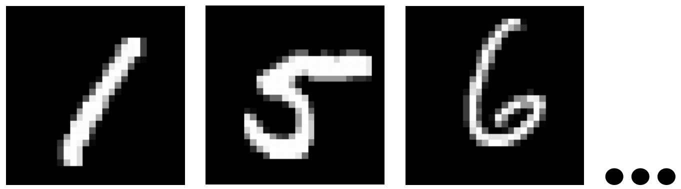

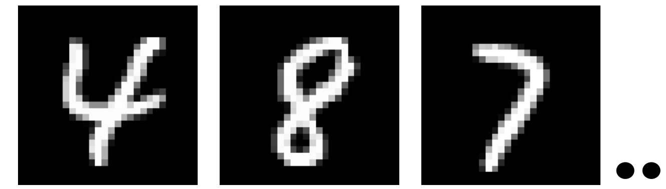

Averaging

$\boldsymbol{\mathcal{B}}(\boldsymbol{x}_k)$

Centroids

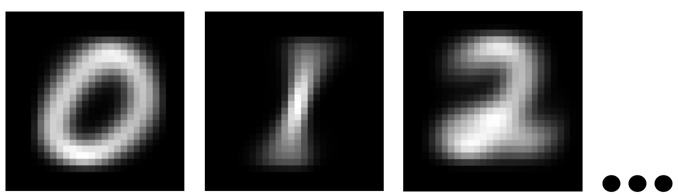

$\boldsymbol{c}_0$ $\boldsymbol{c}_1$ $\boldsymbol{c}_2$

$\boldsymbol{\mathcal{B}}(\boldsymbol{c}_i)$

$$\hat{\ell}_k := \arg\max_{i=0..9} s_i$$

with $s_i = \langle \mathrm{sign}\, \underbrace{\boldsymbol{\mathcal{B}}(\boldsymbol{c}_i)}_{\text{sketched centroids}}, \boldsymbol{\mathcal{B}}(\boldsymbol{x}_k)\rangle$

$n = 784$	Direct	$m = 400$	$m = 800$	$m = 1600$	$m = 3200$
Acc. [%]	82.1	59.2	66.9	71.8	75.0

Experiments III

Variation

(60 000) Training set — Sketching $\boldsymbol{\mathcal{B}}(\boldsymbol{x}_i)$ — Averaging

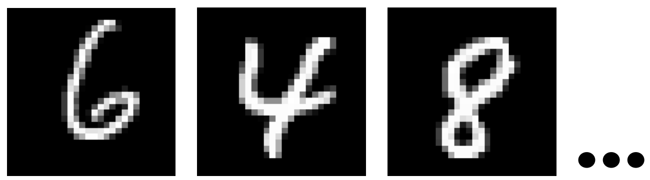

$$\longrightarrow \boldsymbol{\mathcal{X}}^{\text{sk}} \longrightarrow \{\boldsymbol{c}_j^{\boldsymbol{\mathcal{B}}}\}_{j=0}^{9}$$

centroids in the sketched domain

(10 000) Test set — Sketching $\boldsymbol{\mathcal{B}}(\boldsymbol{x}_k)$

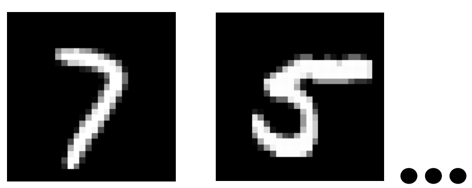

$$\longrightarrow \hat{\ell}_k := \arg\max_j \langle \operatorname{sign}(\boldsymbol{c}_j^{\boldsymbol{\mathcal{B}}}), \boldsymbol{\mathcal{B}}(\boldsymbol{x}_k) \rangle$$

Assumption: ∃ an image whose sketch is $c_j^{\mathscr{B}}$

	Direct	$m = 1\,000$	$m = 10\,000$
Accuracy	82.1%	82.7%	83.9%

Kernelization?

To conclude ...

Take away messages:

- (1) Fluorescent speckle imaging (with MCF) follows a ROP-ed interferometric sensing model
  - Theory + proof-of-concept experiments
- (2) "Signal processing" in the ROP domain is possible
  - Localizing & classifying OPU sketching

To conclude ...

Take away messages:

- (1) Fluorescent speckle imaging (with MCF) follows a ROP-ed interferometric sensing model
  - Theory + proof-of-concept experiments
- (2) "Signal processing" in the ROP domain is possible
  - Localizing & classifying OPU sketching

Open questions:

- (1) More advanced sparsity models; 3D imaging?
- (2) Time filtering? Centroid estimation?
  Usage in compressive learning?

Thank you for your attention!

- O. Leblanc, M. Hofer, S. Sivankutty, H. Rigneault, L. Jacques (2023). "Interferometric lensless imaging: rank-one projections of image frequencies with speckle illuminations". Submitted to IEEE TCI, arXiv:2306.12698.
- R. Delogne, V. Schellekens, L. Daudet, L. Jacques, Signal Processing With Optical Quadratic Random Sketches, ICASSP 2023.
- S. Guérit, S. Sivankutty, J. A. Lee, H. Rigneault and L. Jacques, "Compressive Imaging through Optical Fiber with Partial Speckle Scanning," under review, 2021.
- Rudin, M., & Weissleder, R. (2003). Molecular imaging in drug discovery and development. *Nature reviews Drug discovery*, *2*(2), 123-131.
- E. R. Andresen, S. Sivankutty, V. Tsvirkun, et al., "Ultrathin endoscopes based on multicore fibers and adaptive optics: status and perspectives," Journal of Biomedical Optics, 2016.
- S. Sivankutty, V. Tsvirkun, O. Vanvincq, et al., "Nonlinear imaging through a fermat's golden spiral multicore fiber," Optics letters, 2018.
- Shin, J., Bosworth, B. T., & Foster, M. A. (2017). Compressive fluorescence imaging using a multi-core fiber and spatially dependent scattering. Optics letters, 42(1), 109-112.
- Chen, Y., Chi, Y., & Goldsmith, A. J. (2015). Exact and stable covariance estimation from quadratic sampling via convex programming. *IEEE Transactions on Information Theory*, *61*(7), 4034-4059.
- Cai, T. T., & Zhang, A. (2015). ROP: Matrix recovery via rank-one projections. The Annals of Statistics, 43(1), 102-138.
- Saade, Alaa, et al. "Random projections through multiple optical scattering: Approximating kernels at the speed of light." 2016 IEEE International Conference on Acoustics, Speech and Signal Processing (ICASSP). IEEE, 2016.
- M. Davenport, P. Boufounos, M. Wakin, R. Baraniuk, Signal Processing with Compressive Measurements, IEEE 2010.

Extra slides

Conditions to get the RIP

H1 Bounded FOV : $\text{supp}\, w \subset [-\frac{L}{2}, \frac{L}{2}] \times [-\frac{L}{2}, \frac{L}{2}]$

H2 Bandlimited f :

→ (H1 & H2) $\boldsymbol{f} \in \mathbb{R}^N$ = sampling of $w(x)f(x)$ over a N pixel grid.

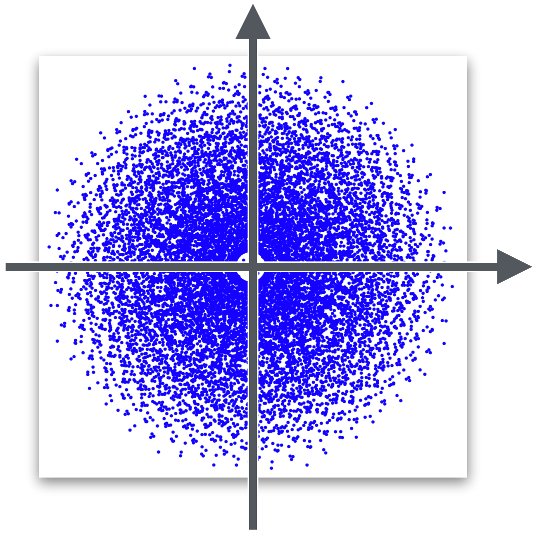

H3 K-sparse $\boldsymbol{f} \in \mathbb{R}^N$ (canonical basis)

H4 Distinct, on-grid, non-zero visibilities

$$|\mathcal{V}_0| \simeq Q^2, \text{ with } \mathcal{V}_0 = \mathcal{V} \setminus \{\mathbf{0}\}$$

H5 RIP Fourier Sensing: For $\boldsymbol{\Phi} \equiv$ partial random Fourier sampling on $\mathcal{V}_0$,

$$\boldsymbol{\Phi} \text{ is RIP}(K, \delta) \text{ if } |\mathcal{V}_0| \gtrsim \delta^{-2} K \text{plog}(N, K, \delta),$$

$$i.e.\ \|\boldsymbol{\Phi u}\|^2 \simeq_\delta \|\boldsymbol{u}\|^2, \ \forall\ K\text{-sparse } \boldsymbol{u} \in \mathbb{R}^N$$

H6 Unit module *sketching vector*: $\boldsymbol{\alpha}_j \sim_{\text{iid}} \boldsymbol{\alpha}_0$, with $|\alpha_k| = 1$.